Supporting Information for
Preparation and Physical Properties of Early-Late Heterobimetallic Compounds Featuring Ir–M Bonds (M = Ti, Zr, Hf)

John J. Curley, Robert G. Bergman, and T. Don Tilley
Department of Chemistry, University of California, Berkeley, CA 94720, U.S.A.

Contents:

Experimental Details

General Considerations

All manipulations were carried out under an atmosphere of purified nitrogen in a Vacuum Atmospheres Nexus glovebox, or by standard Schlenk techniques.[1,2] Inside the glovebox the ambient temperature ranged from 18–22 °C. All glassware was oven-dried at a temperature above 100 °C for at least 3 hours and allowed to cool under dynamic vacuum prior to use. Celite, alumina, and 4 Å sieves were activated by heating to a temperature greater than 180 °C under a dynamic vacuum for 2 d (celite) or 5 d (alumina and 4 Å sieves). Et_2O, *n*-hexane, *n*-pentane, CH_2Cl_2, THF, benzene, and toluene were bubble degassed with nitrogen and forced, under positive pressure, through a column of activated alumina.[3] All solvents were stored over 4 Å sieves. C_6D_6 was degassed under a dynamic vacuum prior to use. CD_2Cl_2 was refluxed over CaH_2 for 24 h then distilled. d_8-THF was distilled from dark purple solutions of sodium benzophenone. ^1H and ^{13}C NMR shifts are referenced against residual solvent resonances (for C_6D_6, 7.16 and 128.4; for d_8-THF, 3.58 and 67.6; for CD_2Cl_2, 5.32 and 54.0 ppm). UV-vis spectra were obtained on a Cary spectrophotometer in 1-cm quartz cells. IR spectroscopy was carried out using a Thermo Scientific iS10 FT-IR spectrometer equipped with either a Smart iTR diamond, ATR accessory, or a solution cell with KBr windows. Raman spectra were acquired using a LabRamHR epi-illumination confocal Raman microscope, manufactured by Horiba Jobin Yvon, in conjunction with a 633 nm, He-Ne laser (1-2 mW) and a CCD detector manufactured by Andor. NMR data were acquired using 600, 500, 400, or 300 MHz spectrometers manufactured by Bruker. Positive-ion ESI-MS were acquired by the QB3 mass spectrometry facility at the University of California, Berkeley using an LTQ FT mass spectrometer, manufactured by Thermo Fisher Scientific, equipped with an electrospray ionization source and a 7 T magnet. Cyclic voltammetry was performed using an EC Epsilon potentiostat manufactured by BASi in conjunction with a glassy carbon working electrode, Pt-wire counter electrode, and Ag-wire pseudo-reference electrode. Combustion analysis was performed by the College of Chemistry Microanalytical Facility at the University of California, Berkeley, or Midwest Microlabs, LLC, Indianpolis, IN. Unless otherwise noted, Teflon-coated magnetic stir bars and magnetic stir plates were used in all reactions. Literature procedures were used for the preparation of Cp*IrN≡^{t}Bu,[4,5], **2**-Zr,[6,7] $Cp_2Hf(^n Bu)_2$,[8] $Cp_2Ti[\eta^2\text{-}C_2(SiMe_3)_2]$,[9] and aromatic azides.[10]

General Remarks on the Determination of Molecular Structure by X-ray Diffraction

X-ray diffraction data were collected using either Bruker AXS three-circle or Bruker AXS Microstar kappa-geometry diffractometers coupled to a CCD detector with graphite-monochromated Mo Kα radiation (λ = 0.71073 Å). The structures were solved by direct methods using SHELXS and refined against F^2 on all data by full-matrix least squares with SHELXL-97.[11] All non-hydrogen atoms were refined anisotropically; all hydrogen atoms were included into the model at their geometrically calculated positions and refined using a riding model. Additional details concerning the data collection, data work-up, and crystallographic solutions for compounds **2**-Ti, **2**-Hf, **3**-Zr, **5**-Hf are contained in the cif files that are available as electronic supplementary material.

A disordered cyclopentadienyl ligand in the structure of **3**-Zr was refined with the help of similarity restraints on 1-2 and 1-3 distances and displacement parameters as well as rigid bond restraints for anisotropic displacement parameters. The ratios were refined freely, while constraining the total occupancy of all components to unity. For the purpose of calculating bond distances and angles between atoms involved in this disorder, only the major component of the disorder was considered.

Preparation of Cp*Ir(μ-N^{t}Bu)TiCp$_2$ (2-Ti)

In the glovebox, a solution of $Cp_2Ti(\eta^2\text{-}C_2(SiMe_3)_2)$ (262 mg, 0.752 mmol, 1.2 equiv) in 10 mL of *n*-hexane was added to solid **1** (250 mg, 0.627 mmol, 1.0 equiv) at 20 °C. The resulting mixture was stirred at 20 °C for 14 h before the solvent was removed by application of a dynamic vacuum. To completely remove the $C_2(SiMe_3)_2$ byproduct, it was necessary to resuspend the mixture in 10 mL of *n*-hexane and subsequently remove solvent from the mixture using a dynamic vacuum, for a second time. The resulting brown powder was washed with *n*-pentane (3 mL × 4) that had been cooled to –35 °C to remove the excess $Cp_2Ti(\eta^2\text{-}C_2(SiMe_3)_2)$. This afforded Cp*Ir(μ-N^{t}Bu)TiCp$_2$ (180 mg, 0.312 mmol, 49.8%) as a bright orange powder.^1H NMR (400 MHz, C_6D_6, 20 ˚C): δ = 6.42 (s, 10 H, Cp), 1.75 (s, 15 H, Cp*), 0.78 (s, 9 H, Cp) ppm. ^{13}C NMR (100 MHz, C_6D_6, 20 ˚C): δ = 114.2 (Cp), 82.4 (C_5–Cp*), 73.5 (CMe$_3$), 32.1 (C(CH$_3$)$_3$), 11.0 (Me_5–Cp*) ppm. UV-vis (Et_2O, 20 °C): λ (ε) = 272 (25400), 295 (23200), 373 (4760) sh nm ($M^{-1}cm^{-1}$). EA calcd for $C_{24}H_{34}IrNTi$: C, 49.99; H, 5.94; N, 2.43; Found: C, 50.08; H, 5.98; N, 2.29%. Crystals suitable for single-crystal X-ray diffraction were grown at –35 ˚C from an *n*-penane/Et_2O solution.

UV-vis data for Cp*Ir(μ-N^{t}Bu)ZrCp$_2$ (2-Zr)

UV-vis (Et_2O, 20 °C): λ (ε) = 296 (11000), 395 (4200) nm ($M^{-1}cm^{-1}$). The preparation and characterization of this compound has been previously reported.[6,7]

Preparation of Cp*Ir(μ-N^{t}Bu)HfCp$_2$ (2-Hf)

As powders, $Cp_2Hf(^n Bu)_2$ (530 mg, 1.25 mmol, 1.0 equiv) and **1** (500 mg, 1.25 mmol, 1.0 equiv) were combined in a 50 mL tube. To the combined solids was added 5 mL of C_6H_6, and the resulting mixture was freeze-pump-thaw degassed three times. This mixture was then heated to 105 °C for 3.5 h without stirring. Then, the mixture was frozen, and the solvent removed by pumping on the frozen solution at 20 °C. This procedure gives Cp*Ir(μ-N^{t}Bu)HfCp$_2$ (730 mg, 1.03 mmol, 82.6%) in greater than 90% purity. Recrystallization of the mixture from Et_2O/*n*-pentane mixtures at –35 °C was inefficient and reduced the yield to (220 mg, 0.310 mmol, 25%). ^1H NMR (500 MHz, C_6D_6, 20 ˚C): 6.08 (s, 10 H, Cp), 1.91 (s, 15 H, Cp*), 1.19 (s, 9 H, ^{t}Bu) ppm. ^{13}C NMR (100 MHz, C_6D_6, 20 ˚C): δ = 110.0 (Cp), 87.8 (C_5–Cp*), 73.9 (CMe$_3$), 33.7 (C(CH$_3$)$_3$), 11.47 (Me_5–Cp*) ppm. UV-vis

(Et_2O, 20 °C): λ (ε) = 293 (8500) sh, 373(4500) nm ($M^{-1}cm^{-1}$). EA calcd for $C_{24}H_{34}HfIrN$: C, 40.76; H, 4.85; N, 1.98; Found: C, 40.60; H, 4.57; N, 2.21%. Crystals suitable for single-crystal X-ray diffraction were grown at –35 ˚C from a Et_2O/THF solution.

Preparation of [Cp_2Fe][OTf][12-14]

AgOTf (3 g, 11.6 mmol, 1 equiv) and Cp_2Fe (2.3 g, 12.4 mmol, 1.07 equiv) were combined as solids and then cooled to –35 °C. Then 40 mL of cold (–35 °C) THF was added to the combined solids forming a brown mixture. The mixture was stirred for 25 min, during which time it became dark blue in color. The mixture was filtered through a Celite pad, and the pad was washed with THF (*ca*. 100 mL) until the washings were colorless. The solvent was then removed using a dynamic vacuum to produce blue powder. This powder was washed with *n*-pentane (50 mL × 2) and Et_2O (20 mL × 3) to remove the excess Cp_2Fe. The washed solids were stored under a dynamic vacuum to remove traces of solvent. The resulting blue powder was collected (3.64 g, 10.8 mmol, 94%). ^{1}H NMR (500 MHz, CD_2Cl_2, 20 ˚C): δ = 33.27 (br s, $\Delta\nu_{1/2}$ = 720 Hz, 10 H, Cp) ppm. ^{19}F NMR (376 MHz, CD_2Cl_2, 20 ˚C): δ = –89.72 ppm. EA calcd for $C_{11}H_{10}F_3FeO_3S$: C, 39.43; H, 3.01; Found: C, 39.24; H, 2.93%. ESI-MS(+): m/z = 186.0125 (186.0126, Cp_2Fe^+).

Preparation of 2,6-lutidinium triflate, [Lut–H][OTf][15,16]

At 20 °C, to a solution of 2,6-lutidine (2.71 g, 25 mmol, 1 equiv) in 25 mL of *n*-pentane was added triflic acid (3.84 g, 25 mmol, 1 equiv) dropwise. Following the addition, the mixture was allowed to stir for 10 min before the white precipitate was collected by filtration. The so obtained solids were washed with Et_2O (10 mL × 3), and stripped of the remaining solvent under a dynamic vacuum to yield the product (4.5 g, 17.5 mmol, 70%). ^{1}H NMR (500 MHz, CD_2Cl_2, 20 ˚C): δ = 14.45 (s, 1 H, N*H*), 8.24 (t, J_{HH} = 8 Hz, 1 H, para-H), 7.57 (d, J_{HH} = 8 Hz, 9 H, meta-H), –8.09 (s, 1 H, μ-H) ppm. ^{13}C NMR (125 MHz, CD_2Cl_2, 20 ˚C): δ = 154.4 (2,6-C), 146.6 (4-C), 125.5 (3,5-C), 121.0 (q, J_{CF} = 320 Hz, *C*F_3) 19.9 (Me) ppm. ^{19}F NMR (376 MHz, CD_2Cl_2, 20 ˚C): δ = –79.4 ppm. EA calcd for $C_8H_{10}F_3NO_3S$: C, 37.35; H, 3.92; N, 5.45; Found: C, 37.35; H, 3.91; N, 5.45%. ESI-MS(+): m/z = 108.08080 (108.08078, $C_7H_{10}N^+$).

Preparation of Cp*Ir(μ-N^{t}Bu)(μ-H)ZrCp$_2$OTf (3-Zr)

At –35 °C, a solution of 2,6-lutidinium triflate (48 mg, 0.187 mmol, 0.95 equiv) in 5 mL THF was added dropwise to a solution of Cp*Ir(μ-N^{t}Bu)ZrCp$_2$ (122 mg, 0.196 mmol, 1 equiv) in 10 mL of THF. During the addition a change in the color of the solution from red to orange was observed. The mixture was stirred for 15 min before the solvent was removed by the application of a dynamic vacuum. The mixture was then stored under a dynamic vacuum for 14 h to evaporate 2,6-lutidine formed during the reaction. The remaining material was washed with *n*-pentane (5 mL × 3). The product was then obtained via crystallization from THF layered with a mixture of 1:1 Et_2O/*n*-pentane at –35 °C as two crops of orange crystals (121 mg, 0.157 mmol, 84%). ^{1}H NMR (400 MHz, d_8-THF, 20 ˚C): 6.08 (s, 10 H, Cp), 1.99 (s, 15 H, Cp*), 1.36 (s, 9 H, ^{t}Bu), –8.08 (s, 1 H, μ-H) ppm. ^{13}C NMR (100 MHz, d_8-THF, 20 ˚C): δ = 111.2 (Cp), 90.0 (*C*$_5$–Cp*), 80.3 (*C*Me$_3$), 31.9 (C(*C*H$_3$)$_3$), 10.51 (*Me*$_5$–Cp*) ppm. ^{19}F NMR (376 MHz, d_8-THF, 20 ˚C): δ = –79.2 ppm. ^{1}H NMR (400 MHz, CD_2Cl_2, 20 ˚C): δ = 6.06 (s, 10 H, Cp), 1.95 (s, 15 H, Cp*), 1.32 (s, 9 H, ^{t}Bu), –8.09 (s, 1 H, μ-H) ppm. ^{19}F NMR (376 MHz, CD_2Cl_2, 20˚C): δ = –78.7 ppm. EA calcd for $C_{25}H_{34}F_3IrNO_3SZr$: C, 39.04; H, 4.46; N, 1.82; Found: C, 38.32; H, 4.25; N, 1.84%. ESI-MS(+): m/z = 620.1442 (620.1440, M^+–OTf).

Alternative Preparation of Cp*Ir(μ-N^{t}Bu)(μ-H)ZrCp$_2$OTf (3-Zr) from Schwartz's Reagent

A solution of Cp*IrN^{t}Bu (100 mg, 0.251 mmol, 1equiv) in 10 mL of CH_2Cl_2 and added to solid $Cp_2Zr(H)Cl$ (75 mg, 0.256 mmol, 1equiv) at 20 °C. This produced a cloudy suspension that was stirred for 5 min before a solution of Me_3SiOTf (56 mg, 0.252 mmol, 1 equiv) in 3 mL CH_2Cl_2 was added. Upon addition of the final reagent, the mixture immediately clarified to form an orange solution. This solution was stirred an additional 10 min before it was filtered through celite and concentrated to *ca*. 2 mL. The solution was layered with *ca*. 10 mL of *n*-pentane and stored at –35 °C to precipitate an orange powder which was collected by filtration. The so-obtained solids were washed with *n*-pentane (5 mL × 3) at 20 °C to afford the product. 124 mg, 0.161, 64%

Preparation of Cp*Ir(μ-N^{t}Bu)(μ-H)HfCp$_2$OTf (3-Hf)

At –35 °C, a solution of 2,6-lutidinium triflate (14 mg, 0.054 mmol, 0.98 equiv) in 2 mL of THF was added dropwise to a solution of Cp*Ir(μ-N^{t}Bu)HfCp$_2$ (39 mg, 0.055 mmol, 1 equiv) in 5 mL of THF. Upon addition of 2,6-lutidinium triflate, the initially red solution became yellow in color. The reaction mixture was stirred for 15 min before the solvent was removed by application of a dynamic vacuum. The so-obtained solids were stored under a dynamic vacuum for 6 h to evaporate the 2,6-lutidine formed in the reaction. The remaining material was washed with *n*-pentane (10 mL × 3) and dissolved in a minimum of THF (*ca*. 2 mL). The THF solution was layered with 10 mL of 1:1 Et_2O/*n*-pentane and stored at –35 °C to afford the product as yellow crystals (34mg, 0.039 mmol, 72%).^{1}H NMR (400 MHz, d_8-THF, 20 ˚C): 6.05 (s, 10 H, Cp), 1.98 (s, 15 H, Cp*), 1.38 (s, 9 H, ^{t}Bu), –7.17 (s, 1 H, μ-H) ppm. ^{13}C NMR (100 MHz, d_8-THF, 20 ˚C): δ = 109.2 (Cp), 93.6 (*C*$_5$–Cp*), 80.2 (*C*Me$_3$), 27.9 (C(*C*H$_3$)$_3$), 9.6 (*Me*$_5$–Cp*) ppm. ^{19}F NMR (376 MHz, d_8-THF, 20 ˚C): δ = –79.1 ppm. ^{1}H NMR (400 MHz, CD_2Cl_2, 20 ˚C): 6.06 (s, 10 H, Cp), 1.95 (s, 15 H, Cp*), 1.32 (s, 9 H, ^{t}Bu), –8.09 (s, 1 H, μ-H) ppm. ^{19}F NMR (376 MHz, CD_2Cl_2, 20 ˚C): δ = –78.9 ppm. EA calcd for $C_{25}H_{35}F_3HfIrNO_3S$: C, 35.02; H, 4.12; N, 1.63; Found: C, 35.17; H, 4.36; N, 1.70%.

General procedure for the preparation of Cp*Ir(μ-N^{t}Bu)(μ-N$_3$C$_6$H$_4$R)HfCp$_2$, R = Me$_2$N, Me, H, Br, CF$_3$

A *ca* 0.01 M solution of the appropriate aryl azide in *n*-pentane was cooled to –35 °C. This solution was then transferred onto solid **2**-Hf, immediately forming a green solution. The solution was stirred for 2 h before the solvent was removed under dynamic vacuum. Storing the green solids under dynamic vacuum for *ca*. 6 h removed the excess aryl azide, leaving only the azide complex, Cp*Ir(μ-N^{t}Bu)(μ-N$_3$C$_6$H$_4$R)HfCp$_2$. The

following lists the amounts used for each procedure: for R=NMe_2, 40 mg, 0.057 mmol, 1 equiv Hf and 9.2 mg, 0.057 mmol, 1.0 equiv azide gave 46 mg, 0.053 mmol, 93%; for 4-Me, 71 mg, 0.10 mmol, 1 equiv Hf and 12 mg, 0.105 mmol, 1.05 equiv azide gave 80 mg, 0.095 mmol, 94%; for 4-H, 80 mg, 0.113 mmol, 1 equiv Hf and 12 mg, 0.117 mmol, 1.05 equiv azide gave 91 mg, 0.110 mmol, 97%; for 4-Br, 40 mg, 0.057 mmol, 1 equiv Hf and 12 mg, 0.060 mmol, 1.05 equiv azide gave 48 mg, 0.052 mmol, 92%; and for 4-CF_3, 40 mg, 0.057 mmol, 1 equiv Hf and 11 mg, 0.058 mmol, 1.05 equiv azide gave 47 mg, 0.051 mmol, 92%.

Characterization Data for Cp*Ir(μ-N^{t}Bu)(μ-$N_3C_6H_4NMe_2$)HfCp$_2$

^{1}H NMR (500 MHz, C_6D_6, 20 °C): 8.10 (d, J_{HH} = 7 Hz, 2 H, *o*-Ar), 6.91 (d, J_{HH} = 7 Hz, 2 H, *m*-Ar), 5.95 (s, 10 H, Cp), 2.73 (s, 6 H, NMe_2), 1.56, (s, 9 H, ^{t}Bu), 1.46 (s, 15 H, Cp*) ppm. ^{13}C NMR (125 MHz, C_6D_6, 20 °C): δ = 148.2 (*ipso*-Ar), 147.5 (Ar), 122.2 (Ar), 114.8 (Ar), 108.4 (Cp), 88.8 (C_5–Cp*), 69.9 (CMe_3), 41.6 ($N(CH_3)_2$), 36.5 ($C(CH_3)_3$), 10.9 (Me_5–Cp*) ppm.

Characterization Data for Cp*Ir(μ-N^{t}Bu)(μ-$N_3C_6H_4Me$)HfCp$_2$

^{1}H NMR (500 MHz, C_6D_6, 20 °C): 8.03 (d, J_{HH} = 8 Hz, 2 H, *o*-tol), 7.35 (d, J_{HH} = 8 Hz, 2 H, *m*-tol), 5.88 (s, 10 H, Cp), 2.34 (s, 3 H, tol-Me), 1.58, (s, 9 H, ^{t}Bu), 1.44 (s, 15 H, Cp*) ppm. ^{13}C NMR (125 MHz, C_6D_6, 20 °C): δ = 153.9 (*ipso*-tol), 132.0 (*ipso*-tol), 130.3 (tol), 121.3 (tol), 108.4 (Cp), 89.0 (C_5–Cp*), 70.2 (CMe_3), 36.4 ($C(CH_3)_3$), 21.6 (tol-Me), 10.7 (Me_5–Cp*) ppm.

Characterization Data for Cp*Ir(μ-N^{t}Bu)(μ-N_3Ph)HfCp$_2$ (5-Hf)

^{1}H NMR (400 MHz, C_6D_6, 20 °C): 8.09 (d, J_{HH} = 7 Hz, 2 H, *o*-Ph), 7.55 (t, J_{HH} = 7 Hz, 2 H, *p*-Ph), 7.17 (t, obscured by residual solvent, 2 H, *m*-Ph), 5.88 (s, 10 H, Cp), 1.57, (s, 9 H, ^{t}Bu), 1.42 (s, 15 H, Cp*) ppm. ^{13}C NMR (100 MHz, C_6D_6, 20 °C): δ = 156.0 (*ipso*-Ph), 129.7 (Ph), 123.0 (Ph), 121.3 (Ph), 108.5 (Cp), 89.1 (C_5–Cp*), 70.4 (CMe_3), 36.5 ($C(CH_3)_3$), 10.8 (Me_5–Cp*) ppm. EA calcd for $C_{30}H_{39}HfIrN_4$: C, 43.60; H, 4.75; N, 6.77; Found: C, 44.0; H, 5.06; N, 5.90%. ESI-MS(+): m/z = 829.2376 (829.2348, MH^+) amu.

Characterization Data for Cp*Ir(μ-N^{t}Bu)(μ-$N_3C_6H_4Br$)HfCp$_2$

^{1}H NMR (600 MHz, C_6D_6, 20 °C): 7.74 (d, J_{HH} = 9 Hz, 2 H, *o*-Ar), 7.58 (d, J_{HH} = 9 Hz, 2 H, *m*-Ar), 5.80 (s, 10 H, Cp), 1.51, (s, 9 H, ^{t}Bu), 1.35 (s, 15 H, Cp*) ppm. ^{13}C NMR (150 MHz, C_6D_6, 20 °C): δ = 155.0 (*ipso*-Ar), 133.2 (Ar), 118.2 (Ar), 115.1 (Ar), 108.6 (Cp), 89.2 (C_5–Cp*), 70.6 (CMe_3), 36.3 ($C(CH_3)_3$), 10.7 (Me_5–Cp*) ppm.

Characterization Data for Cp*Ir(μ-N^{t}Bu)(μ-$N_3C_6H_4CF_3$)HfCp$_2$

^{1}H NMR (600 MHz, C_6D_6, 20 °C): 7.89 (d, J_{HH} = 8 Hz, 2 H, *o*-Ar), 7.74 (d, J_{HH} = 8 Hz, 2 H, *m*-Ar), 5.82 (s, 10 H, Cp), 1.53, (s, 9 H, ^{t}Bu), 1.37 (s, 15 H, Cp*) ppm. ^{13}C NMR (150 MHz, C_6D_6, 20 °C): δ = 158.8 (*ipso*-Ar), 126.92 (q, J = Hz, Ar), 125.8 (Ar), 123.3 (q, J_{CF} = 320 Hz, CF_3), 108.7 (Cp), 89.5 (C_5–Cp*), 70.9 (CMe_3), 36.3 ($C(CH_3)_3$), 10.7 (Me_5–Cp*) ppm. One ^{13}C resonance was not located, presumably because it is obscured by the resonance for C_6D_6. ^{19}F NMR (376 MHz, C_6D_6, 20 °C): δ = –60.8 ppm.

Preparation of Cp*Ir(μ-N^{t}Bu)(μ-NPh)HfCp$_2$ (5-Hf)

A 0.6 mL C_6D_6 solution of 45 mg(0.054 mmol) Cp*Ir(μ-N^{t}Bu)(μ-N_3Ph)HfCp$_2$ was heated to 120 °C for 6 h. After this time the mixture was analyzed by ^{1}H NMR spectroscopy which indicated that the starting material had been consumed and conversion to the desired product proceeded in >90%. The material was crystallized from *n*-pentane/Et_2O mixtures at –35 °C in two crops. 36 mg, 0.045, 83% ^{1}H NMR (600 MHz, C_6D_6, 20 °C): δ = 7.36 (d, J_{HH} = 8 Hz, 2 H, *o*-Ph), 6.95 (t, J_{HH} = 8 Hz, 1 H, *p*-Ph), 6.91 (t, J_{HH} = 8 Hz, 2 H, *m*-Ph), 5.81 (s, 10 H, Cp), 1.71, (s, 9 H, ^{t}Bu), 1.20 (s, 15 H, Cp*) ppm. ^{13}C NMR (100 MHz, C_6D_6, 20 °C): δ = 168.2 (*ipso*-Ph), 128.3 (Ph), 125.9 (Ph), 120.1 (Ph), 109.3 (Cp), 87.1 (C_5–Cp*), 68.4 (CMe_3), 36.7 ($C(CH_3)_3$), 11.0 (Me_5–Cp*) ppm.

Formation of Cp*Ir(μ-N^{t}Bu)(μ-NC_6H_4R)HfCp$_2$ by N_2 Extrusion from Cp*Ir(μ-N^{t}Bu)(μ-$N_3C_6H_4R$)HfCp$_2$ (R = NMe_2, Me, Br, CF_3)

The procedure described for the preparation of **5**-Hf was followed for each compound in this series.

Characterization Data for Cp*Ir(μ-N^{t}Bu)(μ-$NC_6H_4NMe_2$)HfCp$_2$

^{1}H NMR (400 MHz, C_6D_6, 20 °C): δ = 6.94 (d, J_{HH} = 8 Hz, 2 H, *o*-Ar), 6.85 (d, J_{HH} = 8 Hz, 2 H, *m*-Ar), 5.86 (s, 10 H, Cp), 3.31 (s, 6 H, NMe_2), 2.76, (s, 9 H, ^{t}Bu), 1.76 (s, 15 H, Cp*) ppm.

Characterization Data for Cp*Ir(μ-N^{t}Bu)(μ-NC_6H_4Me)HfCp$_2$

^{1}H NMR (500 MHz, C_6D_6, 20 °C): δ = 6.96 (d, J_{HH} = 8 Hz, 2 H, *o*-tol), 6.87 (d, J_{HH} = 8 Hz, 2 H, *m*-tol), 5.83 (s, 10 H, Cp), 2.44 (s, 3 H, tol-Me), 1.73, (s, 9 H, ^{t}Bu), 1.22 (s, 15 H, Cp*) ppm.

Characterization Data for Cp*Ir(μ-N^{t}Bu)(μ-NC_6H_4Br)HfCp$_2$

^{1}H NMR (300 MHz, C_6D_6, 20 °C): δ = 7.62 (d, J_{HH} = 9 Hz, 2 H, *o*-Ar), 6.61 (d, J_{HH} = 9 Hz, 2 H, *m*-Ar), 5.74 (s, 10 H, Cp), 1.65, (s, 9 H, ^{t}Bu), 1.13 (s, 15 H, Cp*) ppm.

Characterization Data for Cp*Ir(μ-N^{t}Bu)(μ-$NC_6H_4CF_3$)HfCp$_2$

^{1}H NMR (300 MHz, C_6D_6, 20 °C): δ = 7.56 (d, J_{HH} = 8 Hz, 2 H, *o*-Ar), 6.70 (d, J_{HH} = 8 Hz, 2 H, *m*-Ar), 5.73 (s, 10 H, Cp), 1.62, (s, 9 H, ^{t}Bu), 1.13 (s, 15 H, Cp*) ppm. ^{19}F NMR (376 MHz, C_6D_6, 20 °C): δ = –60.4 ppm.

Kinetics Measurements for 4-Hf → 5-Hf

A stock solution of **2**-Hf (2.5 mmol) in d_{12}-mesitylene was prepared and *ca.* 1 equiv of 1,3,5-trimethoxybenzene was added as an internal standard. An aliquot of the solution was transferred to a J. Young tube which was sealed with a Teflon screw-cap under *ca*. 1 atm of N_2. The sample was transported to a 500 MHZ NMR spectrometer at 20 °C and inserted into a pre-warmed probe. Temperatures from 105 to 135 °C were studied, and the probe temperature was determined by use of a neat ethylene glycol sample. The sample was given 5 min to ensure that the temperature had reach equilibrium before kinetics measurements began. To obtain kinetic information, single-scan ^{1}H NMR spectra were obtained in either 5 or 10 min intervals, and the relative concentration of **4**-Hf was determined by integration of the Cp resonance, which decreases in intensity with time. The resonances corresponding to **5**-Hf increased with time. However, following the concentration of **5**-Hf as a function of time did not

produce useful kinetic information due to the fact that **5**-Hf precipitates from the reaction mixture. The integrals for the added 1,3,5-trimethoxybenzene were invariant with respect to time at all temperatures studied. For complexes $Cp^*Ir(\mu\text{-}N^tBu)(\mu\text{-}N_3C_6H_4R)HfCp_2$ (R = Me_2N, Me, Br, CF_3), the kinetic measurements were carried out in an identical fashion at 130 °C. The reaction kinetics were monitored for no fewer than 3 half-lives, except for when the total length of the required run made this inconvenient. Specifically, 1 and 2.6 half-lives of data were obtained at 105 and 115 °C, respectively, and 2.4 half-lives for $Cp^*Ir(\mu\text{-}^tBu)(\mu\text{-}N_3C_6H_4NMe_2)HfCp_2$ at 130 °C. This experiment was repeated using a solution containing 12.5 mmol of **5**-Hf at 130 °C, and identical kinetic behavior was observed.

Preparation of $Cp^*Ir(\mu\text{-}N^tBu)(\mu\text{-}S)HfCp_2$ (6-Hf)

At 20 °C, an 8 mL solution of **2**-Hf (45 mg, 0.070 mmol, 1 equiv) in C_6H_6 was added to a 2 mL C_6H_6 slurry of S_8 (2.25 mg, 0.0088 mmol, 0.126 equiv). The resulting mixture was stirred for 30 min before it is filtered twice through a glass fiber and the solution frozen. C_6H_6 was removed from the frozen solution to yield a green solid (43.5 mg, 0.064 mmol, 92%). ^{1}H NMR (500 MHz, C_6D_6, 20 °C): 5.73 (s, 10 H, Cp), 1.73 (s, 9 H, ^{t}Bu), 1.50 (s, 15 H, Cp*) ppm. ^{13}C NMR (125 MHz, C_6D_6, 20 °C): δ = 109.4 (Cp), 88.7 (C_5–Cp*), 72.2 (CMe$_3$), 36.2 (C(CH$_3$)$_3$), 11.36 (Me_5–Cp*) ppm. ESI-MS: m/z = 742.1610 (742.1579, MH^+) amu.

General Remarks Regarding Computational Methods

Density functional theory (DFT) calculations were performed using the Gaussian09 software package.[17] The basis set SDD was used for Hf, Ir, Ti, and Zr with effective core potentials,[18-20] whereas 6-31G* was used for all other atoms.[21,22] Both hybrid functional B3LYP[23-26] and pure DFT functional PW91PW91[27-31] were used for calculations involving **1**-M (M = Ti, Zr, Hf). While only B3LYP was used for **2**-Zr. Optimized geometries for these compounds are given in Tables S4–S7. All geometry optimization procedures were initiated from atomic coordinates of single-crystal X-ray structures, and the resulting optimized geometries were subjected to vibrational frequency calculations to ensure that these correspond to a minimum on the potential energy surface.

DFT Vibrational Frequency Analysis for 2-M

Optimized geometries for **2**-M were subjected to vibrational frequency analysis that also predicted Raman intensity using the Gaussian09 package.[17] Predominantly metal-metal stretching modes were located by inspection of the atomic displacements for each mode, and were visualized using the Gaussian09 package. A comparison of the energies between the DFT-predicted and experimentally assigned vibrations are shown in Table 3. These energies are not corrected and no scaling factor was used.

Table 3. DFT Predicted Ir–M Stretching Modes for **2**-M.

2-M	experimental	B3LYP	PW91PW91
Ti	238	279.02	280.95
Zr	153	189.18	185.57
Hf	—	164.26	168.99

TDDFT Calculations for 2-M

The first 50 singlet-to-singlet electronic excited states were calculated for each **2**-M using the TDDFT[32-36] implementation provided with the Gaussian09 software package.[17] Both the pure DFT functional PW91PW91[27-31] and the hybrid functional B3LYP[23-26] were used. Molecular orbital contour plots were generated from the Gaussian checkpoint file that was written by the calculation using the B3LYP functional. The first 50 electronic excited states for **2**-Ti and the first 20 electronic excited states for **2**-Zr and **2**-Hf are listed below.

DFT Calculated ^{1}H NMR shifts for 3-Zr

The NMR shifts were predicted using the gauge-independent atomic orbital method[37-41] as it is implemented by the NMR prediction utility[42-44] that is packaged with Gaussian09.[17] This method provided chemical shielding tensors for the hydrogen atoms contained in **3**-Zr. The calculated chemical shielding tensors of individual hydrogen atoms were averaged for each the Cp, Cp*, and ^{t}Bu ligand. The chemical shift tensors for the Cp* ligand was used as the reference signal, and the chemical shift set to 1.99 ppm, the value found in d_8-THF. This led to the predicted shifts of 6.06, 1.24, and –4.39 ppm for the Cp, ^{t}Bu, and hydride ligands, respectively.

DFT Vibrational Freuqency Analysis for 3-Zr

A vibrational frequency analysis was performed by the Gaussian09 computational package.[17] A single vibration was found that only displaced the hydride ligand, while the atomic positions of other atoms were virtually unchanged. This vibrational mode corresponds to an energy of 2047.5 cm^{-1}.

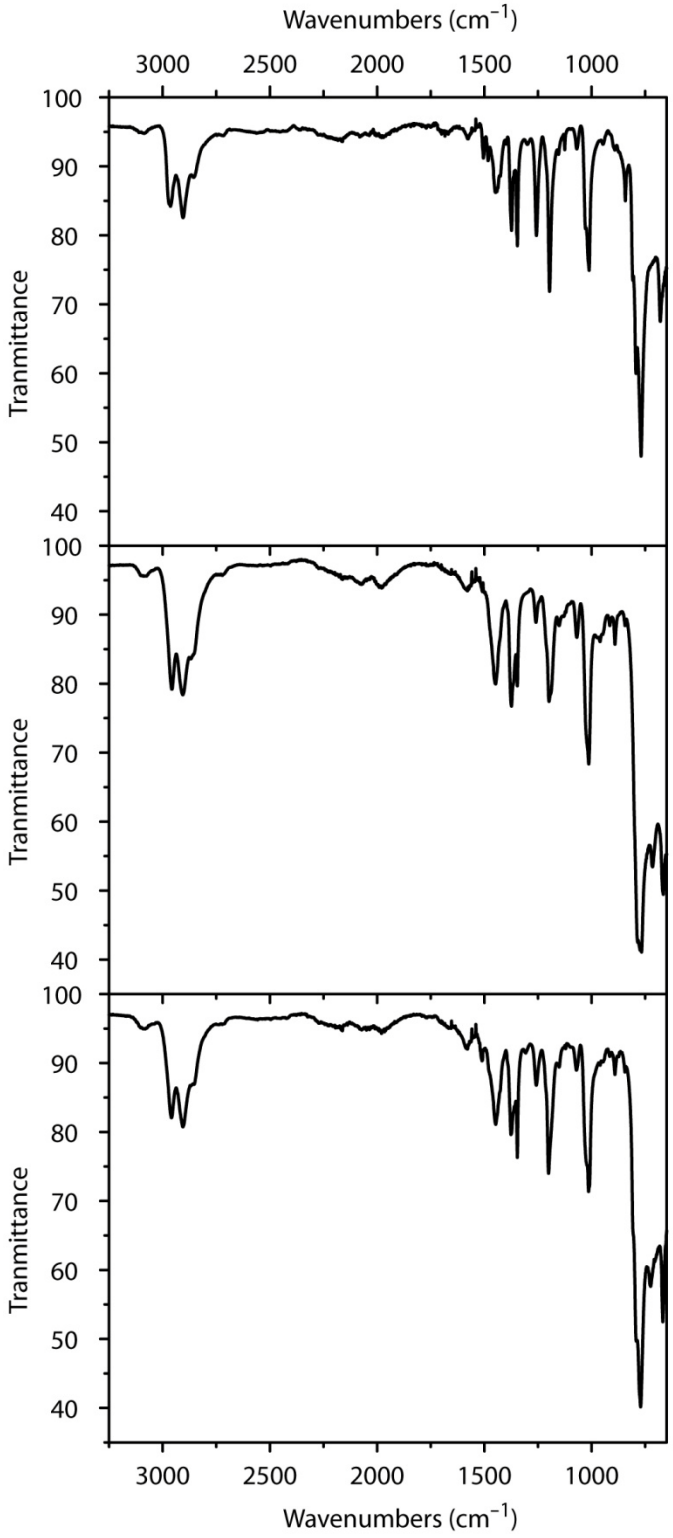

Figure S1. ATR-IR spectroscopy data for Cp*Ir(μ-N^{t}Bu)MCp$_2$ (**2**-M).

Table S1. Solid-state (ATR) IR Data for Cp*Ir(μ-N^{t}Bu)MCp$_2$ (**2**-M).

Ti		Zr		Hf	
Position (cm^{-1})	Transmittance	Position (cm^{-1})	Transmittance	Position (cm^{-1})	Transmittance
3088	94.77	3088	95.58	3088	94.95
2964	84.21	2957	79.19	2959	82.07
2905	82.55	2906	78.39	2906	80.75
2855	88.40	2869	83.59	2869	86.70
1505	91.18	1509	93.38	1511	90.32
1447	86.21	1447	79.95	1447	81.10
1373	80.70	1374	76.74	1376	79.62
1346	78.47	1346	79.68	1346	76.30
1257	79.97	1259	88.90	1258	86.78
1196	71.87	1199	77.41	1201	74.01
1069	92.53	1069	86.71	1071	88.96
1012	74.92	1013	68.34	1014	71.36
948	93.20	915	88.40	915	90.95
891	92.36	891	85.71	891	88.34
843	85.00	844	88.42	845	88.69
808	73.48	785	41.36	808	65.90
793	59.97	774	42.48	792	49.69
769	47.97	767	41.08	771	40.16
—	—	716	53.44	725	57.62
680	67.52	666	49.43	668	52.48

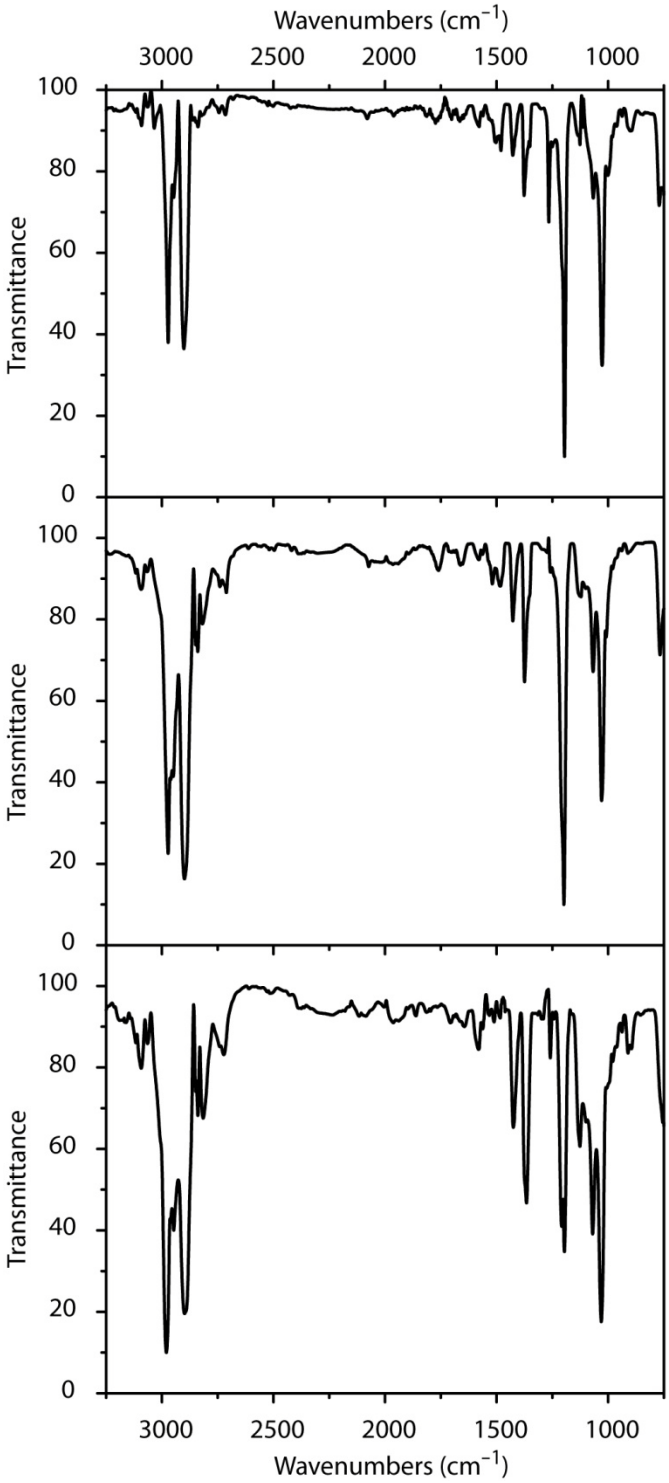

Figure S2. Solution infrared spectroscopy data for Cp*Ir(μ-N^{t}Bu)MCp$_2$ (**2**-M) in C_6D_6 using a KBr cell.

Table S2. Solution (C_6D_6) IR Data for Cp*Ir(μ-N^{t}Bu)MCp$_2$ (**2**-M).

Ti		Zr		Hf	
Position (cm^{-1})		Position (cm^{-1})		Position (cm^{-1})	
3092	(w)	3093	(w)	3093	(w)
2972	(s)	2972	(s)	2980	(s)
2947	(m)	2949	(m)	2947	(m)
2900	(s)	2899	(s)	2898	(s)
1427	(w)	1427	(w)	1425	(m)
1376	(m)	1374	(m)	1366	(m)
1266	(m)	1211	(m)	1209	(m)
1195	(s)	1198	(s)	1196	(s)
1066	(m)	1067	(m)	1069	(m)
1027	(s)	1029	(s)	1030	(s)

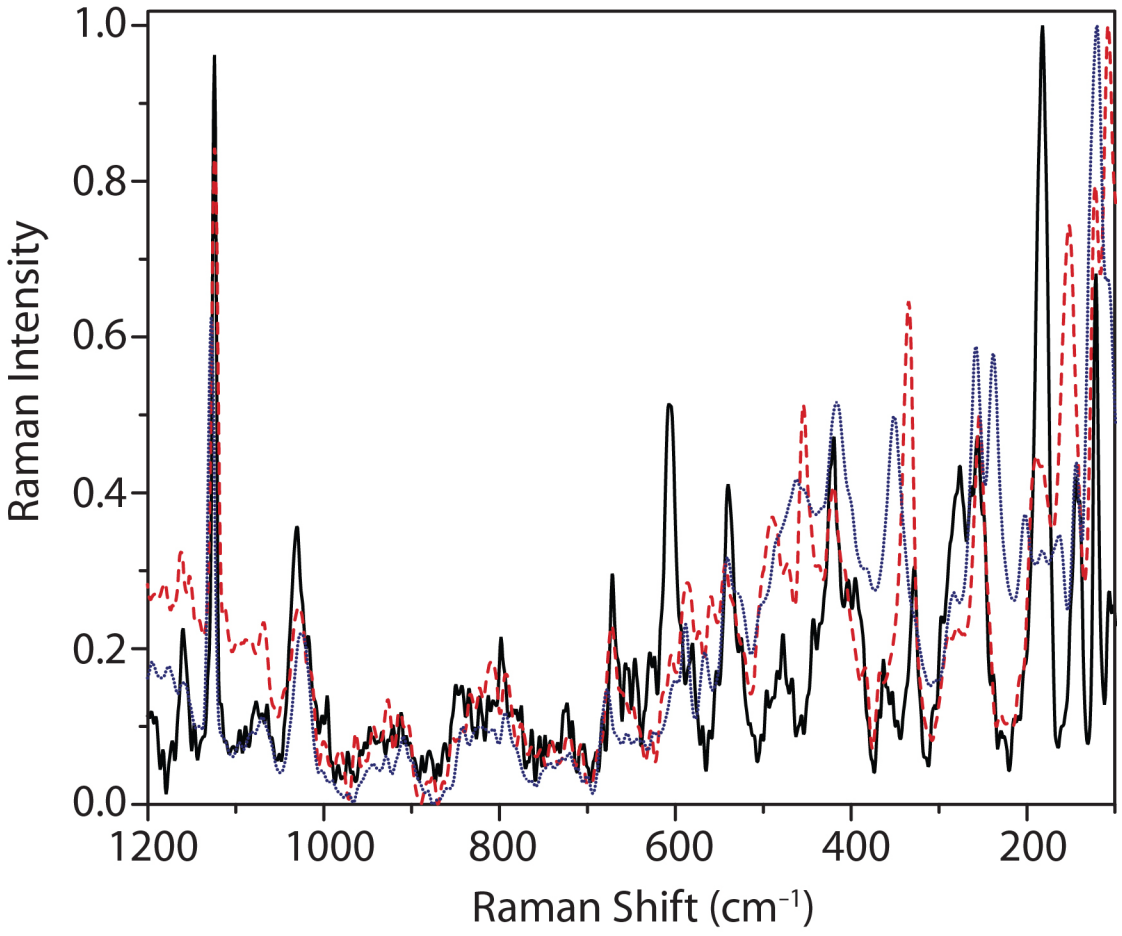

Figure S3. Raman spectra (λ_{ex} = 633nm) of **2**-Ti (·····), **2**-Zr (----), and **2**-Hf (——) as powders at 20 °C are shown from 1200–100 cm^{-1}.

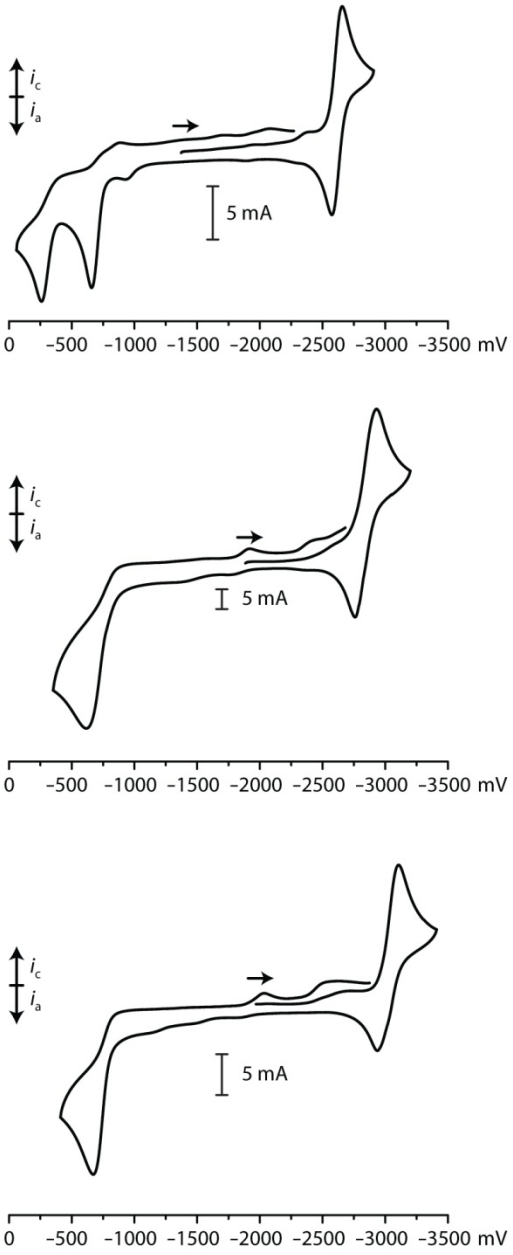

Figure S4. Cyclic voltammetry data for Cp*Ir(μ-N^{t}Bu)MCp$_2$ (**2**-M) are shown from Ti (top) to Zr (middle) to Hf (bottom). Data acquired in 0.1 M [N^{n}Bu$_4$][PF$_6$]/THF solution at 20 °C. Potentials are shown in reference to $Cp_2Fe^{0/+}$.

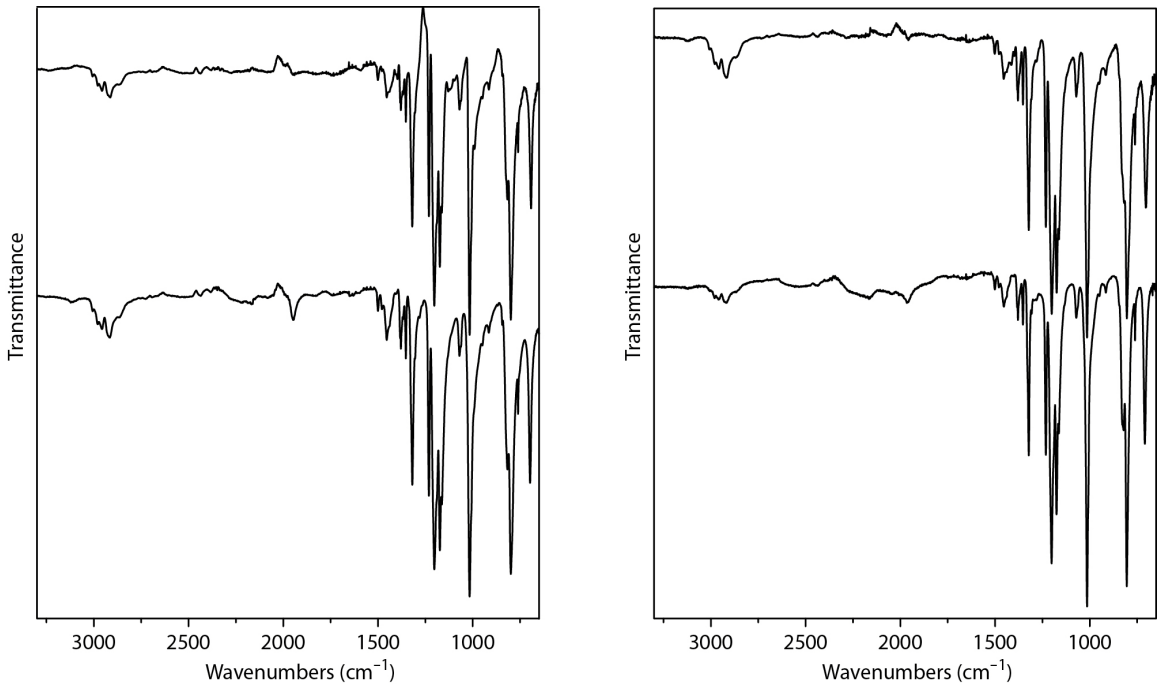

Figure S5. Infrared spectra (ATR) for Cp*Ir(μ-N^{t}Bu)(μ-D)ZrCp$_2$OTf (above) and Cp*Ir(μ-N^{t}Bu)(μ-H)ZrCp$_2$OTf (**3**-Zr, below) are shown on the left, while those for Cp*Ir(μ-N^{t}Bu)(μ-D)HfCp$_2$OTf (above) and Cp*Ir(μ-N^{t}Bu)(μ-H)HfCp$_2$OTf (**3**-Hf, below) are shown on the right.

Table S3. Infrared spectral data for Cp*Ir(μ-N^{t}Bu)(μ-H)MCp$_2$OTf and Cp*Ir(μ-N^{t}Bu)(μ-D)MCp$_2$OTf (M = Zr, Hf).

Cp*Ir(μ-N^{t}Bu)(μ-H)ZrCp$_2$OTf		Cp*Ir(μ-N^{t}Bu)(μ-D)ZrCp$_2$OTf		Cp*Ir(μ-N^{t}Bu)(μ-H)HfCp$_2$OTf		Cp*Ir(μ-N^{t}Bu)(μ-D)HfCp$_2$OTf	
Position (cm^{-1})	Transmittance	Position (cm^{-1})	Transmittance	Position (cm^{-1})	Transmittance	Position (cm^{-1})	Transmittance
2915	87	2913	94	2919	95	2919	93
1948	91	—	—	1966	95	—	—
1454	86	1454	94	1454	94	1454	93
1379	84	1379	91	1379	92	1379	90
1353	82	1353	88	1353	91	1353	89
1319	52	1319	63	1322	70	1322	71
1231	49	1231	66	1232	70	1232	71
1203	32	1203	45	1202	53	1201	58
1173	37	1173	54	1176	61	1175	61
1070	82	1070	91	1071	92	1071	90
1016	26	1016	38	822	74	1015	55
				805	49	804	57
				761	89	761	83
				709	72	705	74

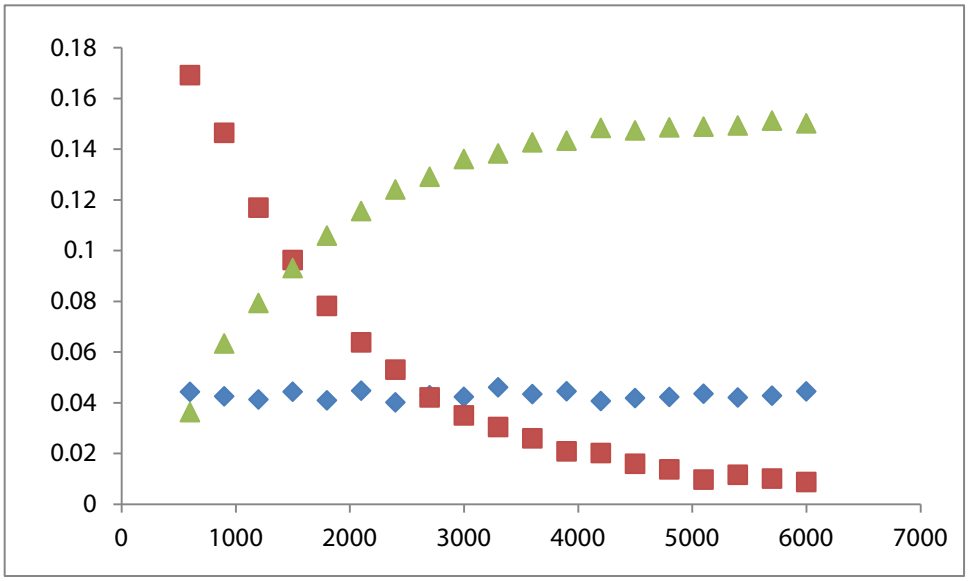

Figure S6. Integral intensities for the ^{1}H NMR signals for Cp resonances of **4**-Hf (squares) and **6**-Hf (triangles), as well as the methyl resonance of 1,3,5-trimethoxybenzene (diamonds) at 130 °C as a function of time.

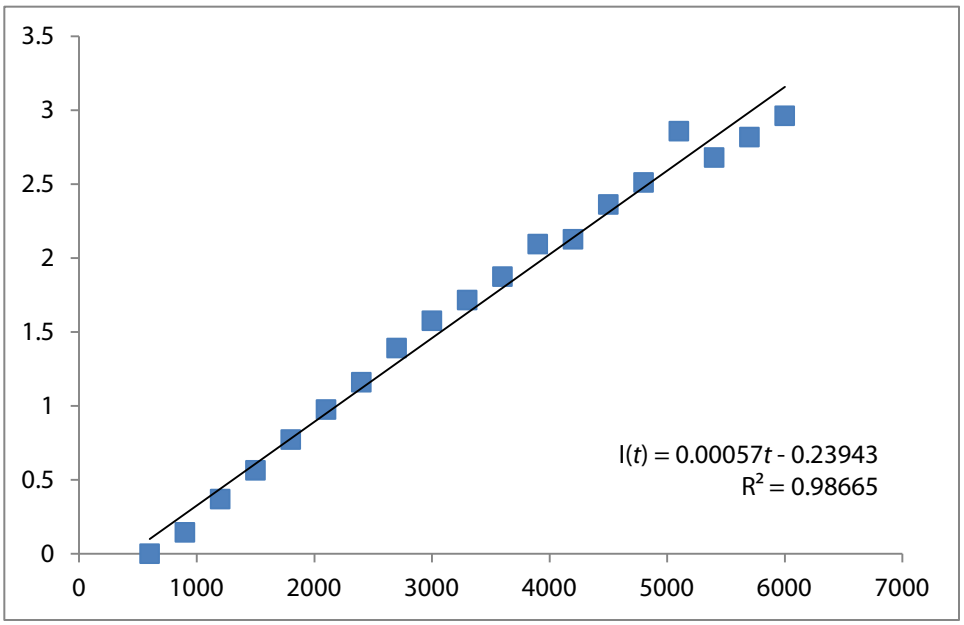

Figure S7. A fit to the natural log of the ^{1}H NMR integral intensity for **4**-Hf as a function of time. The fit that is shown was used to determine the rate constant at 130 °C.

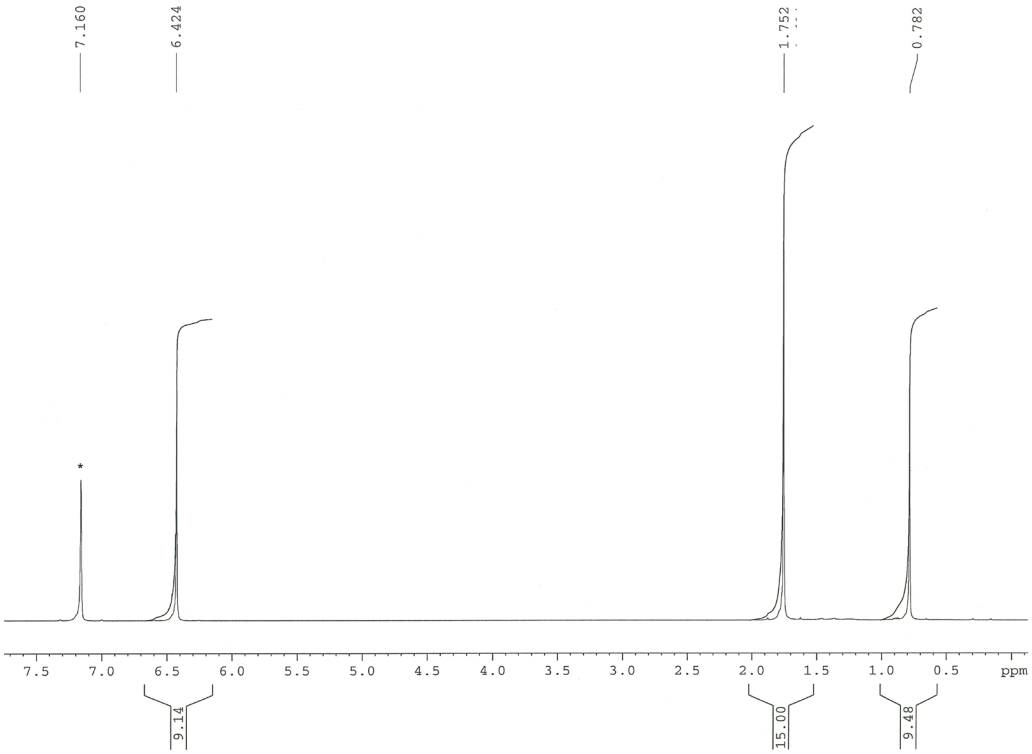

Figure S8. ^{1}H NMR (400 MHz, C_6D_6, 20 °C) spectrum of Cp*Ir(μ-N^{t}Bu)TiCp$_2$ (**2**-Ti).

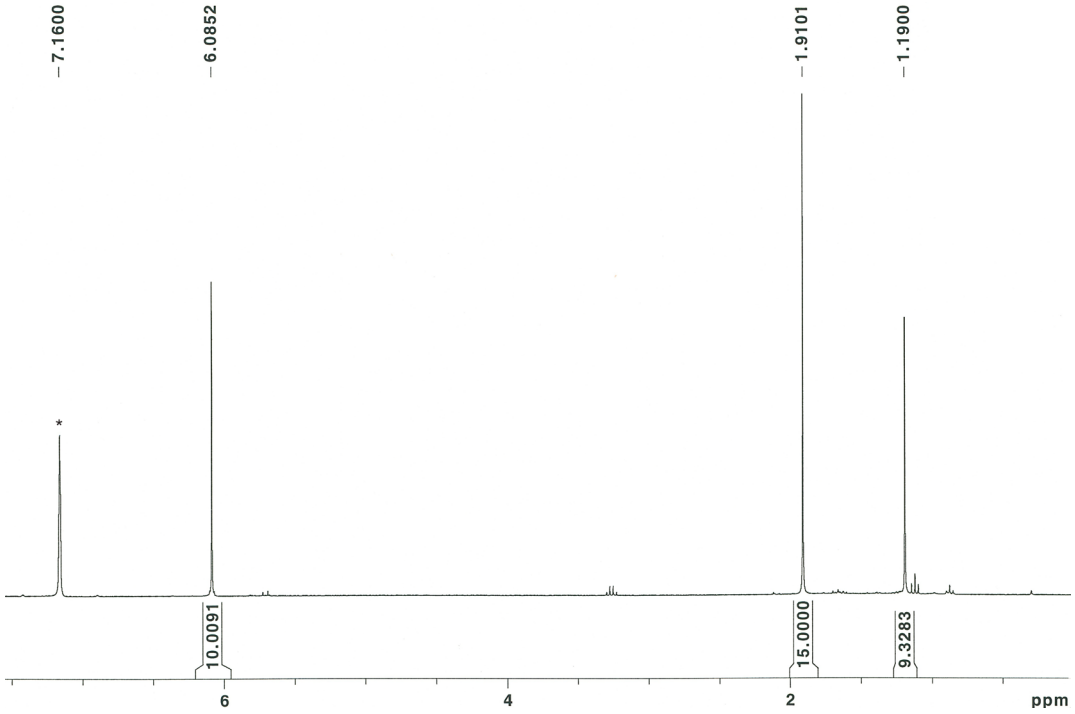

Figure S9. ^{1}H NMR (400 MHz, C_6D_6, 20 °C) spectrum of Cp*Ir(μ-N^{t}Bu)HfCp$_2$ (**2**-Hf).

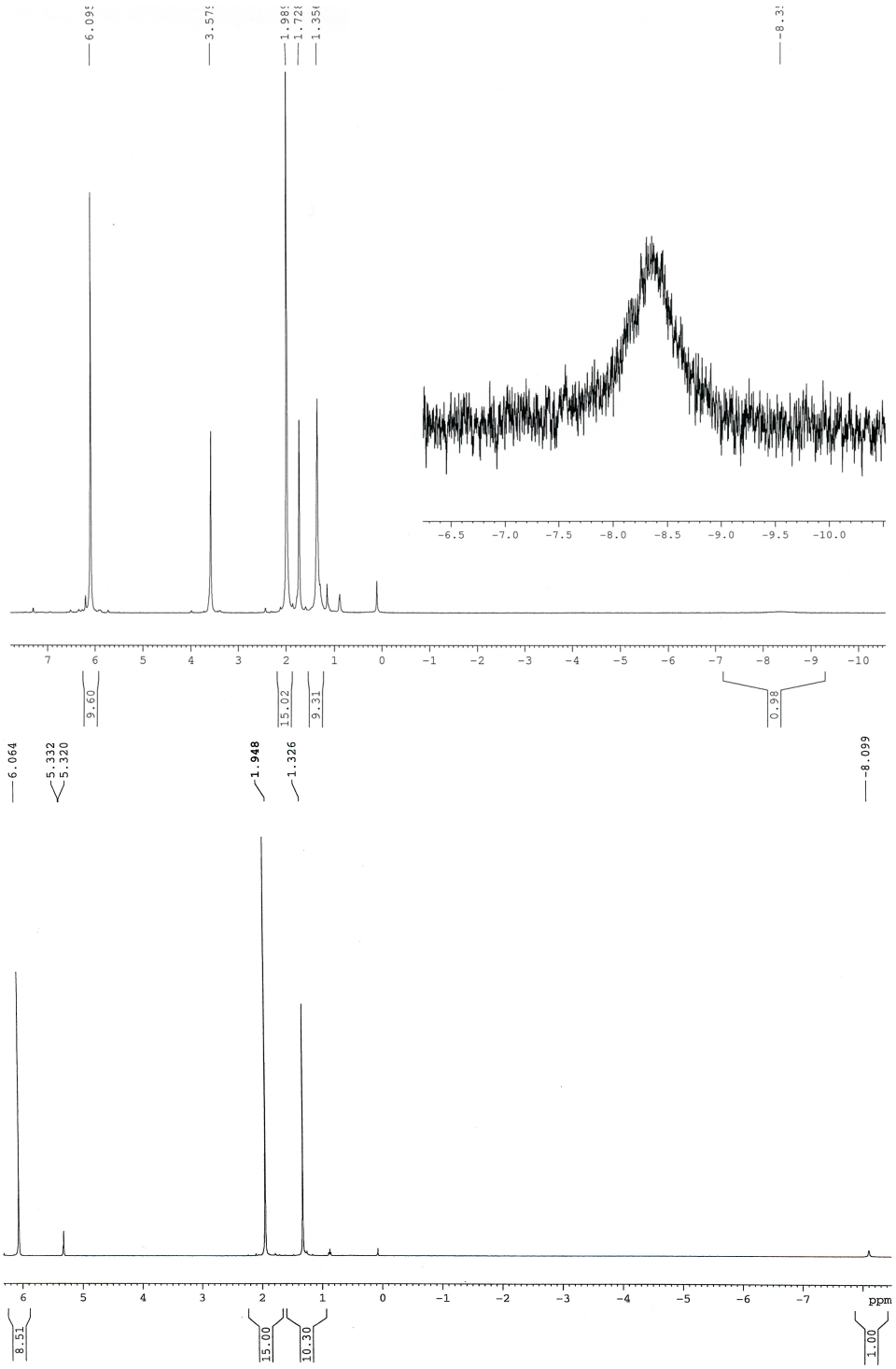

Figure S10. ^{1}H NMR (500 MHz, 20 °C) spectrum of Cp*Ir(μ-N^{t}Bu)(μ-H)ZrCp$_2$OTf (**3**-Zr) in d_8-THF (top) and CD_2Cl_2. (bottom).

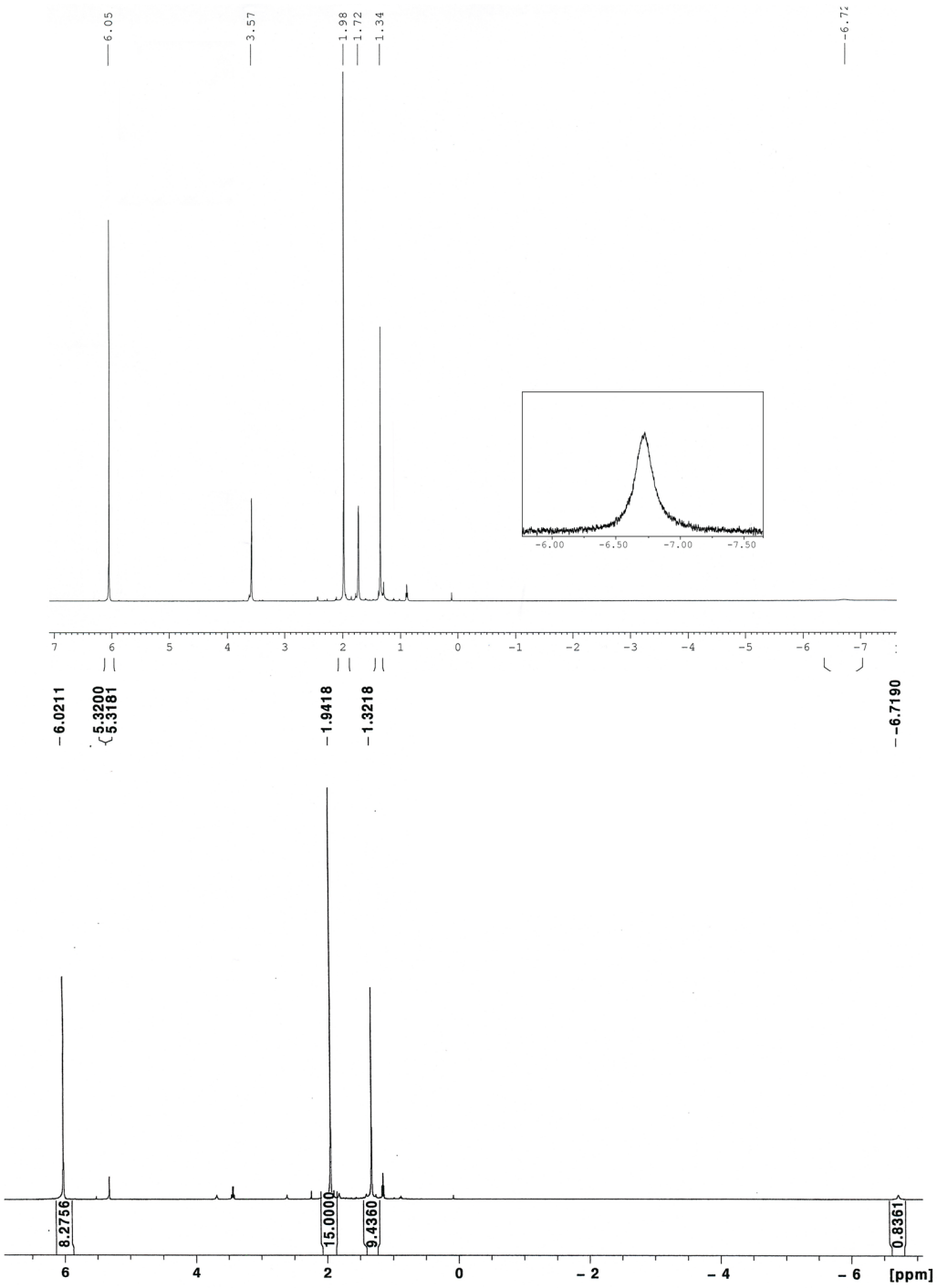

Figure S11. ^{1}H NMR (500 MHz, 20 °C) spectrum of Cp*Ir(μ-N^{t}Bu)(μ-H)HfCp$_2$OTf (**3**-Hf) in d_8-THF (top) and CD_2Cl_2 (bottom).

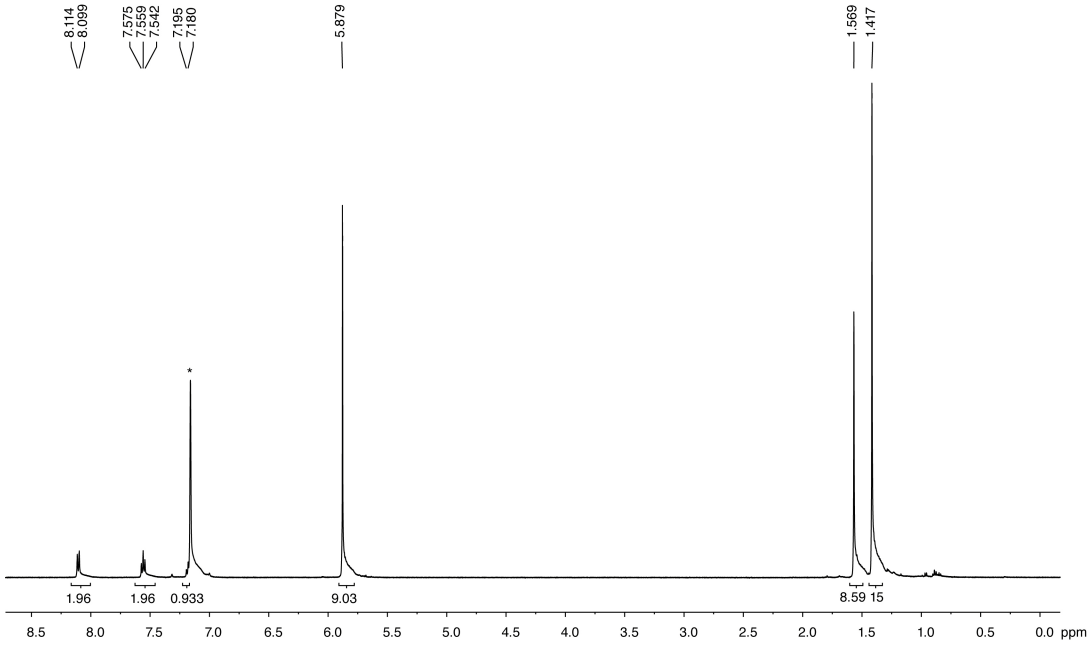

Figure S12. ^{1}H NMR (300 MHz, C_6D_6, 20 °C) spectrum of Cp*Ir(μ-N^{t}Bu)(μ-N_3Ph)HfCp$_2$ (**4**-Hf).

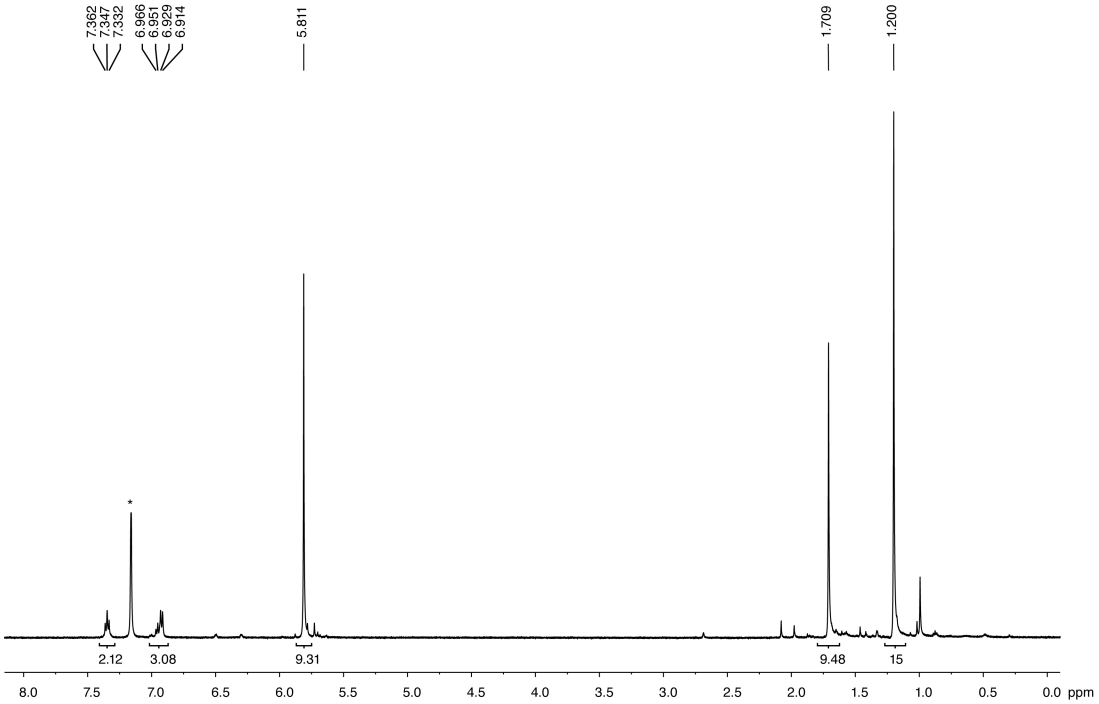

Figure S13. ^{1}H NMR (500 MHz, C_6D_6, 20 °C) spectrum of Cp*Ir(μ-N^{t}Bu)(μ-NPh)HfCp$_2$ (**5**-Hf).

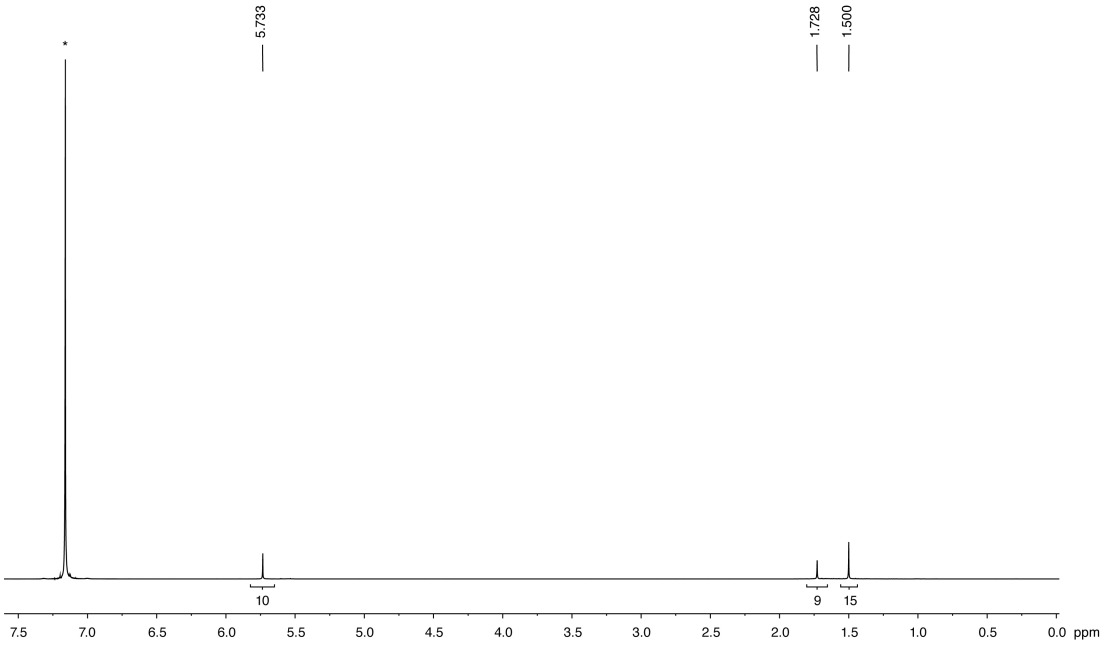

Figure S14. ^{1}H NMR (500 MHz, C_6D_6, 20 °C) spectrum of Cp*Ir(μ-N^{t}Bu)(μ-S)HfCp$_2$ (**6**-Hf).

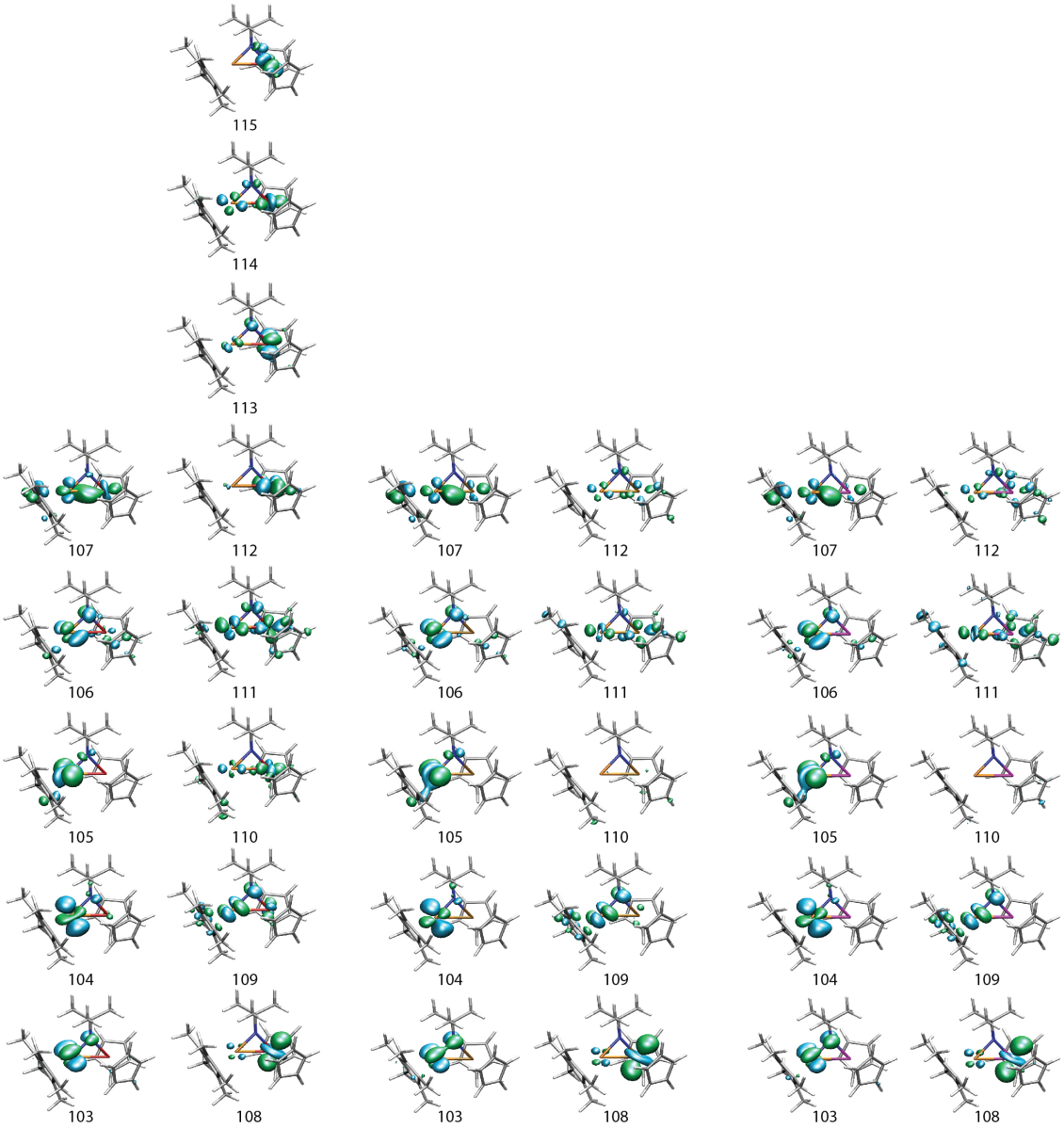

Figure S15. Orbital contour plots for **2**-Ti (left), **2**-Zr (center), and **2**-Hf (right), calculated using the B3LYP functional. In each case, orbital 107 is the HOMO and orbital 108 is the LUMO. These orbitals were rendered at an isosurface value of 0.04, except for orbitals 110–112 for **2**-Zr and **2**-Hf. Because these orbitals are delocalized they were rendered at a value of 0.08. In particular, for both **2**-Zr and **2**-Hf orbital 110 is highly delocalize and contains density in the C-H bonds of the Cp and Cp* ligands.

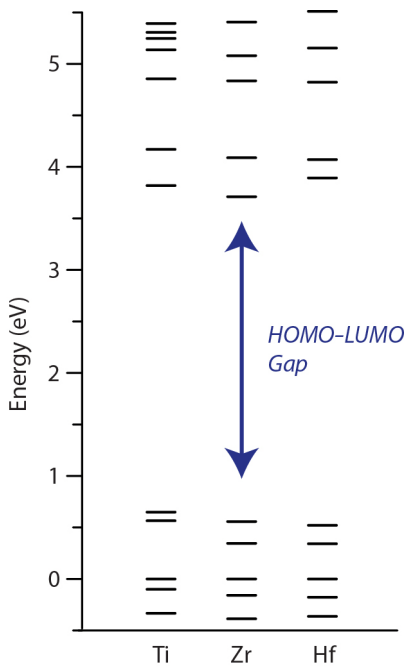

Figure 16. Frontier orbital enegies for Cp*Ir(μ-N^{t}Bu)MCp$_2$ (**2**-M). For each, the energy of orbital 105 is arbitrarily set to 0 eV because this has little contribution from the group 4 metal.

Table S4. Optimized geometries for Cp*Ir(μ-N^{t}Bu)TiCp$_2$ (**2**-Ti) in Cartesian coordinates (Å).

	B3LYP			PW91PW91		
Atom	x	y	z	x	y	z
Ir	–0.7028	–0.0032	–0.0314	–0.6926	–0.0132	–0.0296
Ti	1.8416	–0.2914	–0.0018	1.8308	–0.2979	–0.0013
N	0.6851	1.2873	–0.0494	0.6811	1.2967	–0.0576
C	0.7075	2.7582	–0.0256	0.6785	2.7673	–0.0388
C	0.1881	3.2476	1.3427	0.1713	3.2437	1.3397
C	2.1449	3.2756	–0.2437	2.1051	3.3033	–0.2837
C	–0.1993	3.3132	–1.1421	–0.2630	3.2981	–1.1392
C	–2.3679	–1.0113	–1.1463	–2.3364	–1.0258	–1.1454
C	–2.3460	–1.4418	–2.5847	–2.3077	–1.4589	–2.5816
C	–2.9887	0.2234	–0.6677	–2.9729	0.2097	–0.6685
C	–3.6002	1.2686	–1.5535	–3.5928	1.2453	–1.5573
C	–2.9382	0.2118	0.7399	–2.9179	0.2045	0.7464
C	–3.4749	1.2489	1.6822	–3.4517	1.2440	1.6857
C	–2.2894	–1.0328	1.1562	–2.2544	–1.0385	1.1693
C	–2.1703	–1.4895	2.5816	–2.1249	–1.4839	2.5959
C	–2.0468	–1.8304	–0.0128	–2.0064	–1.8445	–0.0033
C	–1.5927	–3.2618	–0.0460	–1.5271	–3.2665	–0.0352
C	2.1619	0.1985	–2.3711	2.1535	0.2278	–2.3398
C	3.4615	0.0684	–1.8177	3.4543	0.0559	–1.7852
C	3.6378	–1.2813	–1.4262	3.5957	–1.3078	–1.4100
C	2.4285	–1.9684	–1.6748	2.3614	–1.9614	–1.6660
C	1.5143	–1.0542	–2.2759	1.4693	–1.0138	–2.2608
C	1.5126	–0.3115	2.4834	1.4942	–0.2677	2.4572
C	2.6844	0.4171	2.1903	2.6700	0.4599	2.1440
C	3.6268	–0.4763	1.6032	3.6150	–0.4473	1.5691
C	3.0269	–1.7577	1.5436	3.0128	–1.7362	1.5364
C	1.7083	–1.6467	2.0571	1.6913	–1.6155	2.0557
H	0.1769	4.3429	1.3875	0.1296	4.3443	1.3843
H	–0.8272	2.8778	1.5102	–0.8353	2.8387	1.5222
H	0.8214	2.8784	2.1549	0.8329	2.8895	2.1444
H	2.8199	2.9008	0.5321	2.8004	2.9378	0.4880
H	2.5321	2.9574	–1.2163	2.4825	2.9786	–1.2652
H	2.1724	4.3706	–0.2126	2.1192	4.4048	–0.2609
H	–0.2145	4.4093	–1.1214	–0.3176	4.3988	–1.1104
H	0.1581	2.9949	–2.1268	0.0921	2.9957	–2.1367
H	–1.2204	2.9447	–1.0175	–1.2721	2.8841	–0.9974
H	–3.3307	–1.8169	–2.8961	–3.2964	–1.8366	–2.8993
H	–2.0865	–0.6118	–3.2482	–2.0437	–0.6248	–3.2490
H	–1.6244	–2.2450	–2.7544	–1.5819	–2.2682	–2.7470
H	–2.9808	1.4619	–2.4343	–2.9656	1.4510	–2.4382
H	–3.7343	2.2177	–1.0279	–3.7473	2.1970	–1.0283
H	–4.5880	0.9496	–1.9134	–4.5779	0.9107	–1.9291
H	–3.6211	2.2112	1.1848	–3.6109	2.2070	1.1794
H	–4.4443	0.9409	2.0973	–4.4188	0.9325	2.1194
H	–2.7979	1.4111	2.5261	–2.7603	1.4181	2.5241
H	–1.8881	–0.6668	3.2450	–1.8371	–0.6501	3.2538
H	–1.4191	–2.2754	2.6899	–1.3681	–2.2733	2.7054
H	–3.1250	–1.8930	2.9463	–3.0818	–1.8873	2.9736
H	–1.0023	–3.4760	–0.9410	–0.9234	–3.4678	–0.9327
H	–0.9736	–3.5084	0.8207	–0.9034	–3.5026	0.8393
H	–2.4505	–3.9489	–0.0435	–2.3750	–3.9754	–0.0381
H	1.7179	1.1088	–2.7453	1.7291	1.1605	–2.7011
H	4.1977	0.8571	–1.7245	4.2125	0.8302	–1.6739
H	4.5210	–1.6940	–0.9593	4.4710	–1.7513	–0.9411
H	2.2326	–3.0116	–1.4598	2.1336	–3.0053	–1.4528
H	0.5172	–1.2815	–2.6164	0.4572	–1.2079	–2.5987
H	0.5932	0.0962	2.8752	0.5657	0.1501	2.8358
H	2.8427	1.4698	2.3793	2.8280	1.5233	2.3102
H	4.6310	–0.2240	1.2897	4.6218	–0.1982	1.2393
H	3.4779	–2.6575	1.1492	3.4631	–2.6479	1.1505
H	0.9833	–2.4462	2.1223	0.9603	–2.4175	2.1320

Table S5. Optimized geometries for Cp*Ir(μ-N^{t}Bu)ZrCp$_2$ (**2**-Zr) in Cartesian coordinates (Å).

	B3LYP			PW91PW91		
Atom	x	y	z	x	y	z
Ir	–0.8453	–0.0284	–0.0261	–0.8465	–0.0264	–0.0357
Zr	1.7910	–0.1901	–0.0043	1.7700	–0.2156	–0.0055
N	0.4416	1.4060	0.0062	0.4275	1.4073	–0.0889
C	0.2800	2.8654	0.0557	0.2821	2.8690	–0.0854
C	1.6592	3.5419	–0.0841	1.6391	3.5149	–0.4357
C	–0.6337	3.3338	–1.0939	–0.7798	3.2957	–1.1176
C	–0.3495	3.2601	1.4077	–0.1577	3.3174	1.3253
C	–2.4062	–1.1862	–1.1403	–2.3833	–1.2781	–1.0572
C	–2.2905	–1.6851	–2.5522	–2.2693	–1.8746	–2.4296
C	–3.2120	–0.0220	–0.7457	–3.1883	–0.0845	–0.7397
C	–3.8825	0.9043	–1.7163	–3.8701	0.7654	–1.7686
C	–3.2233	0.0431	0.6497	–3.1863	0.0845	0.6575
C	–3.9106	1.0546	1.5190	–3.8523	1.1662	1.4533
C	–2.4159	–1.0758	1.1554	–2.3696	–0.9981	1.2377
C	–2.3016	–1.4397	2.6076	–2.2231	–1.2494	2.7098
C	–2.0546	–1.9147	0.0446	–2.0120	–1.9193	0.1801
C	–1.4989	–3.3085	0.1164	–1.4218	–3.2901	0.3436
C	2.6291	0.4719	2.3606	2.6655	0.6576	2.2432
C	1.5690	–0.4364	2.5948	1.5714	–0.1819	2.5941
C	1.9692	–1.7102	2.1147	1.9102	–1.5168	2.2371
C	3.2953	–1.5989	1.6142	3.2306	–1.5127	1.6922
C	3.6996	–0.2473	1.7494	3.6951	–0.1667	1.6851
C	2.7272	–1.7425	–1.8606	2.6261	–1.8613	–1.7722
C	3.7971	–0.8591	–1.5775	3.7369	–1.0064	–1.5270
C	3.4007	0.4475	–1.9705	3.3879	0.3030	–1.9708
C	2.1024	0.3608	–2.5398	2.0796	0.2443	–2.5351
C	1.6769	–0.9864	–2.4655	1.6005	–1.0876	–2.4092
H	2.3277	3.2285	0.7254	2.4105	3.2080	0.2900
H	2.1254	3.2747	–1.0384	1.9693	3.2045	–1.4393
H	1.5710	4.6335	–0.0445	1.5738	4.6148	–0.4211
H	–0.1898	3.0890	–2.0645	–0.4752	2.9941	–2.1320
H	–0.7932	4.4178	–1.0525	–0.9280	4.3879	–1.1060
H	–1.6020	2.8307	–1.0293	–1.7363	2.8011	–0.8911
H	–0.4765	4.3466	1.4816	–0.2902	4.4107	1.3688
H	–1.3279	2.7838	1.5171	–1.1089	2.8309	1.5890
H	0.2831	2.9298	2.2382	0.5930	3.0277	2.0769
H	–2.0847	–0.8686	–3.2506	–2.0814	–1.1027	–3.1912
H	–3.2216	–2.1704	–2.8773	–3.1988	–2.4009	–2.7134
H	–1.4874	–2.4199	–2.6507	–1.4498	–2.6060	–2.4807
H	–3.2187	1.1635	–2.5471	–3.2089	0.9701	–2.6247
H	–4.1971	1.8359	–1.2387	–4.1910	1.7320	–1.3547
H	–4.7774	0.4392	–2.1514	–4.7684	0.2611	–2.1672
H	–4.1952	1.9472	0.9555	–4.1468	2.0149	0.8192
H	–4.8263	0.6405	1.9626	–4.7635	0.7957	1.9558
H	–3.2707	1.3762	2.3470	–3.1852	1.5546	2.2387
H	–2.1558	–0.5524	3.2306	–2.1403	–0.3058	3.2694
H	–3.2116	–1.9445	2.9612	–3.0969	–1.7957	3.1092
H	–1.4597	–2.1133	2.7848	–1.3268	–1.8474	2.9278
H	–0.8767	–3.4493	1.0044	–0.7742	–3.3453	1.2306
H	–0.8846	–3.5430	–0.7569	–0.8129	–3.5731	–0.5278
H	–2.3079	–4.0518	0.1606	–2.2125	–4.0538	0.4605
H	2.6349	1.5223	2.6198	2.7185	1.7348	2.3910
H	0.6020	–0.1917	3.0080	0.6178	0.1466	2.9985
H	1.3730	–2.6138	2.1409	1.2739	–2.3921	2.3627
H	3.8830	–2.4009	1.1871	3.7774	–2.3827	1.3325
H	4.6618	0.1616	1.4678	4.6688	0.1744	1.3366
H	2.7190	–2.8107	–1.6800	2.5744	–2.9253	–1.5412
H	4.7379	–1.1239	–1.1140	4.6707	–1.2897	–1.0453
H	3.9986	1.3466	–1.8811	4.0195	1.1891	–1.9082
H	1.5184	1.1874	–2.9191	1.5185	1.0832	–2.9401
H	0.7318	–1.3728	–2.8170	0.6323	–1.4501	–2.7424

Table S6. Optimized geometries for Cp*Ir(μ-N^{t}Bu)HfCp$_2$ (**2**-Hf) in Cartesian coordinates (Å).

	B3LYP			PW91PW91		
Atom	x	y	z	x	y	z
Ir	–1.01582	–0.03158	–0.01986	–1.0143	–0.0364	–0.0272
Hf	1.610589	–0.14913	–0.00317	1.5997	–0.1666	–0.0033
N	0.265094	1.429252	–0.05194	0.2496	1.4252	–0.0965
C	0.067979	2.884653	–0.05477	0.0641	2.8820	–0.1133
C	1.429749	3.589843	–0.22424	1.4061	3.5606	–0.4616
C	–0.85933	3.291143	–1.2172	–0.9997	3.2668	–1.1598
C	–0.5674	3.314273	1.284038	–0.3992	3.3392	1.2872
C	–2.57098	–1.22758	–1.09014	–2.5436	–1.2811	–1.0524
C	–2.45287	–1.76969	–2.48617	–2.4180	–1.8784	–2.4236
C	–3.41183	–0.07513	–0.72826	–3.3707	–0.0993	–0.7397
C	–4.10335	0.802824	–1.72836	–4.0534	0.7413	–1.7753
C	–3.41971	0.033279	0.6614	–3.3768	0.0714	0.6549
C	–4.12127	1.057663	1.503385	–4.0565	1.1469	1.4473
C	–2.57555	–1.04542	1.199556	–2.5444	–0.9981	1.2409
C	–2.44301	–1.35571	2.662761	–2.4018	–1.2438	2.7144
C	–2.203	–1.9141	0.11529	–2.1760	–1.9205	0.1879
C	–1.6272	–3.29756	0.22422	–1.5930	–3.2940	0.3557
C	2.60424	0.657641	2.260631	2.5170	0.7537	2.2150
C	1.506634	–0.16075	2.621265	1.4454	–0.1024	2.5921
C	1.803698	–1.49091	2.228599	1.8038	–1.4353	2.2427
C	3.1066	–1.50355	1.657589	3.1169	–1.4121	1.6818
C	3.598219	–0.17429	1.664462	3.5540	–0.0570	1.6501
C	2.390112	–1.79489	–1.8635	2.4867	–1.8332	–1.7392
C	3.566455	–1.07819	–1.53485	3.5933	–0.9735	–1.4948
C	3.363816	0.281599	–1.88707	3.2425	0.3329	–1.9454
C	2.078709	0.392833	–2.48897	1.9384	0.2662	–2.5213
C	1.47167	–0.8856	–2.46907	1.4624	–1.0671	–2.3879
H	2.107487	3.32533	0.594681	2.1791	3.2881	0.2760
H	1.901595	3.297054	–1.16829	1.7547	3.2426	–1.4566
H	1.314714	4.679621	–0.22745	1.3102	4.6583	–0.4667
H	–0.41804	3.009291	–2.17897	–0.6840	2.9458	–2.1648
H	–1.03251	4.373802	–1.22181	–1.1671	4.3562	–1.1749
H	–1.82113	2.779934	–1.12467	–1.9487	2.7609	–0.9265
H	–0.72479	4.398859	1.316877	–0.5601	4.4293	1.3143
H	–1.53133	2.814428	1.416018	–1.3401	2.8319	1.5492
H	0.077142	3.034102	2.123681	0.3517	3.0795	2.0496
H	–2.27255	–0.9717	–3.21288	–2.2326	–1.1055	–3.1850
H	–3.37417	–2.28749	–2.78828	–3.3415	–2.4129	–2.7118
H	–1.63278	–2.48773	–2.56672	–1.5919	–2.6026	–2.4694
H	–3.43687	1.070079	–2.5547	–3.3809	0.9676	–2.6173
H	–4.46228	1.731308	–1.27688	–4.4053	1.6972	–1.3615
H	–4.97126	0.292832	–2.16768	–4.9313	0.2187	–2.1950
H	–4.46242	1.908266	0.907449	–4.3697	1.9863	0.8095
H	–5.00274	0.629447	1.999467	–4.9581	0.7646	1.9581
H	–3.46787	1.446052	2.291542	–3.3916	1.5515	2.2264
H	–2.33414	–0.44223	3.254766	–2.3204	–0.2977	3.2701
H	–3.32807	–1.88886	3.037567	–3.2761	–1.7891	3.1144
H	–1.56944	–1.98215	2.856898	–1.5050	–1.8397	2.9355
H	–1.02352	–3.41388	1.1285	–0.9682	–3.3599	1.2582
H	–0.99025	–3.53685	–0.63174	–0.9656	–3.5744	–0.5033
H	–2.42619	–4.05192	0.263745	–2.3904	–4.0542	0.4483
H	2.686703	1.722561	2.433909	2.5502	1.8334	2.3485
H	0.578286	0.177517	3.057868	0.4917	0.2126	3.0068
H	1.159295	–2.35011	2.360187	1.1858	–2.3198	2.3874
H	3.622965	–2.37352	1.274289	3.6741	–2.2752	1.3220
H	4.565721	0.1501	1.303818	4.5145	0.2989	1.2809
H	2.226973	–2.8554	–1.71296	2.4358	–2.8951	–1.4995
H	4.446975	–1.48382	–1.05576	4.5236	–1.2494	–1.0026
H	4.080149	1.084305	–1.75987	3.8725	1.2201	–1.8859
H	1.629756	1.299594	–2.86907	1.3796	1.0994	–2.9406
H	0.490084	–1.12909	–2.84651	0.4977	–1.4359	–2.7243

Table S7. Optimized geometry for Cp*Ir(μ-N^{t}Bu)(μ-H)ZrCp$_2$OTf (**3**-Zr) in Cartesian coordinates (Å), computed using the B3LYP functional.

Atom	x	y	z
Ir	1.9617	0.1618	0.0281
Zr	–0.8644	–1.0166	0.0836
H	1.1926	–1.2587	0.2340
N	0.2098	0.9115	–0.0331
O	–2.6946	0.2462	–0.1808
O	–4.4084	0.2426	–1.9855
O	–4.7531	–1.1485	0.0928
S	–4.1642	0.0297	–0.5564
C	–4.9084	1.4976	0.3119
F	–4.6391	1.4409	1.6285
F	–4.4034	2.6364	–0.1759
F	–6.2316	1.4985	0.1435
C	–0.2118	2.3261	–0.1791
C	0.9777	3.2961	–0.1642
C	–0.9494	2.4997	–1.5268
C	–1.1297	2.7012	1.0065
C	3.8982	0.0046	1.1630
C	3.9422	–0.9671	0.1100
C	3.8327	–0.2667	–1.1358
C	3.8599	1.1662	–0.8542
C	3.9019	1.3323	0.5565
C	4.0471	–0.2649	2.6321
C	4.0744	–2.4536	0.2824
C	3.8990	–0.8723	–2.5073
C	4.0043	2.2277	–1.9050
C	4.1089	2.6065	1.3208
C	–2.1115	–2.4742	1.8172
C	–2.2630	–1.1520	2.2944
C	–0.9867	–0.6600	2.6680
C	–0.0437	–1.6983	2.4563
C	–0.7314	–2.8156	1.9141
C	–1.1268	–3.2934	–1.1825
C	–2.1719	–2.4657	–1.6499
C	–1.5853	–1.4051	–2.4058
C	–0.1881	–1.5621	–2.3708
C	0.1059	–2.7215	–1.5894
H	1.5344	3.2137	0.7715
H	0.6153	4.3258	–0.2560
H	1.6534	3.0994	–0.9980
H	–0.2779	2.2483	–2.3554
H	–1.2620	3.5427	–1.6505
H	–1.8342	1.8686	–1.5884
H	–1.9972	2.0478	1.0680
H	–1.4837	3.7320	0.8942
H	–0.5716	2.6380	1.9474
H	3.6860	–1.2617	2.8969
H	3.4899	0.4615	3.2293
H	5.1013	–0.2051	2.9346
H	5.1314	–2.7484	0.2889
H	3.5870	–2.9994	–0.5294
H	3.6321	–2.7915	1.2229
H	4.9389	–0.9401	–2.8543
H	3.3478	–0.2715	–3.2353
H	3.4792	–1.8808	–2.5219
H	3.8329	3.2276	–1.5030
H	3.3089	2.0748	–2.7351
H	5.0202	2.2075	–2.3208
H	5.1608	2.6931	1.6240
H	3.5047	2.6364	2.2318
H	3.8625	3.4870	0.7256
H	–2.9103	–3.0988	1.4423
H	–3.1897	–0.5994	2.3159
H	–0.7691	0.3284	3.0465

H	1.0157	–1.6403	2.6572
H	–0.2869	–3.7694	1.6631
H	–1.2452	–4.1928	–0.5942
H	–3.2293	–2.6164	–1.4830
H	–2.1349	–0.6035	–2.8792
H	0.5402	–0.9018	–2.8185
H	1.0902	–3.1248	–1.3954

First 50 Excited States for 2-Ti as Predicted by TDDFT Using PW91PW91

```
Excited State   1:      Singlet-A      1.5373 eV  806.52 nm  f=0.0002  <S**2>=0.000
    106 ->108        -0.14151
    107 ->108         0.69184

Excited State   2:      Singlet-A      1.6050 eV  772.50 nm  f=0.0003  <S**2>=0.000
    106 ->108         0.69172
    107 ->108         0.14184

Excited State   3:      Singlet-A      2.0539 eV  603.67 nm  f=0.0007  <S**2>=0.000
    105 ->108         0.70520

Excited State   4:      Singlet-A      2.2691 eV  546.40 nm  f=0.0006  <S**2>=0.000
    106 ->109        -0.28864
    107 ->109         0.63201

Excited State   5:      Singlet-A      2.3619 eV  524.92 nm  f=0.0020  <S**2>=0.000
    103 ->108         0.17116
    104 ->108         0.46737
    106 ->109         0.43745
    107 ->109         0.21153

Excited State   6:      Singlet-A      2.3914 eV  518.45 nm  f=0.0107  <S**2>=0.000
    103 ->108         0.11809
    104 ->108         0.45828
    106 ->109        -0.45436
    107 ->109        -0.19820

Excited State   7:      Singlet-A      2.4352 eV  509.13 nm  f=0.0018  <S**2>=0.000
    103 ->108         0.66766
    104 ->108        -0.19293

Excited State   8:      Singlet-A      2.6835 eV  462.02 nm  f=0.0030  <S**2>=0.000
    104 ->109        -0.11175
    105 ->109         0.69646

Excited State   9:      Singlet-A      2.8928 eV  428.60 nm  f=0.0004  <S**2>=0.000
    104 ->109         0.68365
    105 ->109         0.10696

Excited State  10:      Singlet-A      3.1211 eV  397.25 nm  f=0.0036  <S**2>=0.000
    103 ->109        -0.14699
```

```
    106 ->110        -0.17887
    106 ->111         0.14343
    107 ->110         0.54712
    107 ->111         0.31603
    107 ->113         0.10073

Excited State  11:      Singlet-A      3.1346 eV  395.54 nm  f=0.0012  <S**2>=0.000
    106 ->110         0.30179
    107 ->110        -0.21250
    107 ->111         0.57806
    107 ->112         0.12675

Excited State  12:      Singlet-A      3.1759 eV  390.39 nm  f=0.0042  <S**2>=0.000
    103 ->109         0.13159
    106 ->110         0.48937
    106 ->111         0.42238
    107 ->110         0.17317
    107 ->111        -0.15485

Excited State  13:      Singlet-A      3.2214 eV  384.88 nm  f=0.0066  <S**2>=0.000
    103 ->109         0.49583
    106 ->110        -0.20079
    106 ->112         0.12326
    107 ->112         0.40023

Excited State  14:      Singlet-A      3.2485 eV  381.67 nm  f=0.0041  <S**2>=0.000
    101 ->108         0.19464
    102 ->108         0.12309
    103 ->109        -0.21270
    106 ->110         0.17074
    106 ->111        -0.29042
    106 ->112        -0.16868
    107 ->110         0.18502
    107 ->111        -0.16578
    107 ->112         0.41592

Excited State  15:      Singlet-A      3.2644 eV  379.81 nm  f=0.0277  <S**2>=0.000
    101 ->108         0.11441
    103 ->109        -0.27777
    106 ->110        -0.22423
    106 ->111         0.39593
    106 ->113         0.16009
    107 ->110        -0.17980
```

```
    107 ->112         0.25210
    107 ->113        -0.22776

Excited State  16:      Singlet-A      3.3028 eV  375.40 nm  f=0.0073  <S**2>=0.000
    101 ->108        -0.15738
    102 ->108         0.50442
    103 ->109        -0.11571
    106 ->112         0.42445

Excited State  17:      Singlet-A      3.3331 eV  371.98 nm  f=0.0002  <S**2>=0.000
    101 ->108         0.10925
    102 ->108         0.45641
    103 ->109         0.14654
    106 ->112        -0.43166
    107 ->112        -0.19621

Excited State  18:      Singlet-A      3.4348 eV  360.97 nm  f=0.0002  <S**2>=0.000
    101 ->108         0.62336
    106 ->112         0.24183
    107 ->112        -0.17727

Excited State  19:      Singlet-A      3.4550 eV  358.85 nm  f=0.0057  <S**2>=0.000
    100 ->108         0.10911
    106 ->113         0.38659
    107 ->113         0.53079
    107 ->114        -0.14300

Excited State  20:      Singlet-A      3.5339 eV  350.84 nm  f=0.0089  <S**2>=0.000
    100 ->108         0.51568
    102 ->108         0.10796
    106 ->113        -0.31460
    106 ->114         0.22178
    107 ->114        -0.24185

Excited State  21:      Singlet-A      3.5666 eV  347.63 nm  f=0.0118  <S**2>=0.000
    100 ->108         0.34475
    105 ->110         0.43485
    106 ->113         0.19815
    106 ->114        -0.10793
    107 ->113        -0.14433
    107 ->114         0.27394
    107 ->115         0.13346
```

```
Excited State  22:      Singlet-A      3.5822 eV  346.11 nm  f=0.0039  <S**2>=0.000
    100 ->108        -0.25380
    105 ->110         0.53496
    105 ->111        -0.14537
    106 ->113        -0.19460
    106 ->114         0.14983
    107 ->114        -0.19185

Excited State  23:      Singlet-A      3.6170 eV  342.78 nm  f=0.0019  <S**2>=0.000
    105 ->110         0.10829
    105 ->111         0.67776
    107 ->114        -0.10848

Excited State  24:      Singlet-A      3.6371 eV  340.89 nm  f=0.0006  <S**2>=0.000
     99 ->108         0.67005
    106 ->114         0.10884

Excited State  25:      Singlet-A      3.6742 eV  337.45 nm  f=0.0077  <S**2>=0.000
     99 ->108        -0.12753
    104 ->112        -0.10869
    106 ->114         0.49265
    106 ->115         0.10260
    107 ->113         0.10686
    107 ->114         0.40657

Excited State  26:      Singlet-A      3.6932 eV  335.71 nm  f=0.0007  <S**2>=0.000
    105 ->112         0.69613

Excited State  27:      Singlet-A      3.7290 eV  332.49 nm  f=0.0027  <S**2>=0.000
    104 ->110         0.22994
    104 ->111         0.10327
    106 ->114         0.11711
    107 ->114        -0.16500
    107 ->115         0.60624

Excited State  28:      Singlet-A      3.7383 eV  331.66 nm  f=0.0002  <S**2>=0.000
    104 ->110         0.64133
    107 ->115        -0.21646

Excited State  29:      Singlet-A      3.7735 eV  328.56 nm  f=0.0005  <S**2>=0.000
    104 ->111         0.65803
    106 ->115        -0.18392
    107 ->115        -0.12392
```

```
Excited State  30:      Singlet-A      3.7901 eV  327.13 nm  f=0.0049  <S**2>=0.000
    104 ->111         0.20700
    106 ->114        -0.18801
    106 ->115         0.62250

Excited State  31:      Singlet-A      3.8409 eV  322.80 nm  f=0.0002  <S**2>=0.000
     98 ->108        -0.42066
    107 ->116         0.55825

Excited State  32:      Singlet-A      3.8464 eV  322.34 nm  f=0.0021  <S**2>=0.000
     98 ->108         0.53054
    107 ->116         0.42955

Excited State  33:      Singlet-A      3.8636 eV  320.90 nm  f=0.0006  <S**2>=0.000
     98 ->108         0.10819
    102 ->109        -0.17275
    104 ->112         0.65199

Excited State  34:      Singlet-A      3.9070 eV  317.34 nm  f=0.0001  <S**2>=0.000
    103 ->110        -0.11012
    105 ->113         0.44290
    106 ->116         0.52529

Excited State  35:      Singlet-A      3.9107 eV  317.04 nm  f=0.0024  <S**2>=0.000
    103 ->110        -0.10720
    105 ->113         0.48977
    105 ->114        -0.11906
    106 ->116        -0.46731

Excited State  36:      Singlet-A      3.9437 eV  314.38 nm  f=0.0039  <S**2>=0.000
    102 ->109         0.66467
    104 ->112         0.15231

Excited State  37:      Singlet-A      3.9778 eV  311.69 nm  f=0.0092  <S**2>=0.000
    101 ->109         0.42841
    103 ->110         0.32762
    103 ->111         0.20567
    105 ->113         0.10310
    106 ->113         0.13609
    106 ->114         0.13704
    107 ->113        -0.12510
    107 ->114        -0.12607
```

```
    107 ->117        -0.10967

Excited State  38:      Singlet-A      3.9803 eV  311.49 nm  f=0.0144  <S**2>=0.000
    101 ->109        -0.26090
    103 ->110         0.47441
    103 ->111         0.30876
    105 ->114        -0.10734
    106 ->113        -0.10625
    107 ->117         0.11517

Excited State  39:      Singlet-A      4.0182 eV  308.56 nm  f=0.0036  <S**2>=0.000
    103 ->110        -0.27443
    103 ->111         0.52258
    103 ->112         0.10073
    104 ->113         0.15400
    107 ->117        -0.29351

Excited State  40:      Singlet-A      4.0375 eV  307.08 nm  f=0.0020  <S**2>=0.000
    103 ->111         0.16923
    103 ->112         0.19463
    104 ->113         0.24219
    107 ->117         0.58756

Excited State  41:      Singlet-A      4.0568 eV  305.62 nm  f=0.0047  <S**2>=0.000
    104 ->113        -0.47381
    105 ->114         0.48609

Excited State  42:      Singlet-A      4.0856 eV  303.47 nm  f=0.0127  <S**2>=0.000
    103 ->112         0.20148
    104 ->113         0.21061
    105 ->114         0.29798
    106 ->117         0.49285
    107 ->117        -0.12939

Excited State  43:      Singlet-A      4.1075 eV  301.85 nm  f=0.0005  <S**2>=0.000
     99 ->109        -0.14363
    103 ->112         0.43721
    104 ->113        -0.32017
    105 ->113        -0.10449
    105 ->114        -0.32019
    106 ->117         0.18815

Excited State  44:      Singlet-A      4.1179 eV  301.09 nm  f=0.0225  <S**2>=0.000
```

```
     99 ->109         0.22404
    100 ->109         0.41467
    103 ->111         0.10165
    103 ->112        -0.25808
    106 ->117         0.35225

Excited State  45:      Singlet-A      4.1351 eV  299.84 nm  f=0.0222  <S**2>=0.000
     99 ->109        -0.16166
    100 ->109         0.53556
    103 ->110         0.10294
    103 ->112         0.17949
    106 ->117        -0.27394

Excited State  46:      Singlet-A      4.2030 eV  294.99 nm  f=0.0137  <S**2>=0.000
    105 ->115         0.67510

Excited State  47:      Singlet-A      4.2142 eV  294.20 nm  f=0.0621  <S**2>=0.000
     99 ->109         0.22158
    101 ->109         0.22873
    104 ->114         0.56424
    105 ->115        -0.13497

Excited State  48:      Singlet-A      4.3125 eV  287.50 nm  f=0.0483  <S**2>=0.000
     99 ->109         0.20603
    103 ->113         0.52348
    104 ->114        -0.21062
    106 ->118         0.10520
    107 ->119         0.14897

Excited State  49:      Singlet-A      4.3280 eV  286.47 nm  f=0.0673  <S**2>=0.000
     99 ->109        -0.19136
    103 ->113         0.40011
    104 ->114         0.21784
    105 ->116         0.17521
    107 ->118         0.32187
    107 ->119        -0.15806

Excited State  50:      Singlet-A      4.3353 eV  285.99 nm  f=0.0029  <S**2>=0.000
     99 ->109         0.10718
    105 ->116         0.67890
    107 ->118        -0.10301
```

First 50 Excited States for 2-Ti as Predicted by TDDFT Using B3LYP

```
Excited State   1:      Singlet-A      1.6084 eV  770.86 nm  f=0.0013  <S**2>=0.000
    100 ->108         0.12298
    106 ->108        -0.23154
    107 ->108         0.63955
Excited State   2:      Singlet-A      2.1848 eV  567.50 nm  f=0.0001  <S**2>=0.000
    106 ->108         0.65013
    107 ->108         0.24778
    107 ->109        -0.10102

Excited State   3:      Singlet-A      2.3783 eV  521.31 nm  f=0.0003  <S**2>=0.000
    106 ->108         0.12071
    106 ->109        -0.10839
    107 ->109         0.67280

Excited State   4:      Singlet-A      2.5023 eV  495.48 nm  f=0.0045  <S**2>=0.000
    103 ->109         0.26679
    106 ->109         0.63247

Excited State   5:      Singlet-A      2.6536 eV  467.23 nm  f=0.0027  <S**2>=0.000
    104 ->109        -0.22785
    105 ->108        -0.19044
    105 ->109         0.61149
    105 ->113         0.10733

Excited State   6:      Singlet-A      2.8174 eV  440.07 nm  f=0.0007  <S**2>=0.000
    104 ->108        -0.39068
    104 ->109         0.50207
    105 ->108        -0.14027
    105 ->109         0.19049

Excited State   7:      Singlet-A      2.8455 eV  435.72 nm  f=0.0006  <S**2>=0.000
    104 ->108        -0.20717
    105 ->108         0.63361
    105 ->109         0.19685

Excited State   8:      Singlet-A      2.9071 eV  426.49 nm  f=0.0022  <S**2>=0.000
    104 ->108         0.50555
    104 ->109         0.39535
    105 ->108         0.15936
    105 ->109         0.13145
```

```
Excited State   9:      Singlet-A      3.0347 eV  408.56 nm  f=0.0003  <S**2>=0.000
    103 ->108         0.12436
    106 ->112        -0.22029
    107 ->112         0.59144
    107 ->113         0.14493
    107 ->114        -0.10261

Excited State  10:      Singlet-A      3.1220 eV  397.13 nm  f=0.0005  <S**2>=0.000
    103 ->108         0.67977
    107 ->112        -0.11635

Excited State  11:      Singlet-A      3.2880 eV  377.08 nm  f=0.0002  <S**2>=0.000
    106 ->113        -0.17501
    107 ->112        -0.15160
    107 ->113         0.61198

Excited State  12:      Singlet-A      3.3668 eV  368.25 nm  f=0.0066  <S**2>=0.000
    103 ->109         0.51164
    106 ->109        -0.21307
    106 ->113         0.30166
    107 ->110         0.16001
    107 ->114         0.12862

Excited State  13:      Singlet-A      3.5166 eV  352.57 nm  f=0.0075  <S**2>=0.000
    106 ->110        -0.14860
    106 ->112        -0.14466
    106 ->113        -0.15742
    106 ->115         0.13769
    107 ->110         0.40370
    107 ->114         0.10067
    107 ->115        -0.36135
    107 ->116         0.20406

Excited State  14:      Singlet-A      3.5729 eV  347.02 nm  f=0.0082  <S**2>=0.000
    106 ->110         0.43617
    106 ->111        -0.31990
    106 ->114         0.32727
    107 ->110         0.20467
    107 ->111        -0.11982

Excited State  15:      Singlet-A      3.6814 eV  336.79 nm  f=0.0026  <S**2>=0.000
    106 ->111        -0.11049
    106 ->112         0.52723
```

```
    107 ->111         0.22534
    107 ->112         0.20741
    107 ->114        -0.14793
    107 ->115        -0.19548
    107 ->116         0.12229

Excited State  16:      Singlet-A      3.7972 eV  326.51 nm  f=0.0029  <S**2>=0.000
     99 ->108        -0.10569
    102 ->108        -0.10555
    106 ->110         0.13369
    106 ->111         0.23685
    106 ->114        -0.12772
    106 ->115        -0.15828
    106 ->116         0.10062
    107 ->110         0.45284
    107 ->114        -0.26134
    107 ->115         0.20875

Excited State  17:      Singlet-A      3.8220 eV  324.40 nm  f=0.0086  <S**2>=0.000
     99 ->108        -0.17984
    100 ->108        -0.15890
    102 ->108        -0.25432
    106 ->110         0.41380
    106 ->111         0.18910
    106 ->112        -0.12043
    106 ->114        -0.15077
    107 ->110        -0.19577
    107 ->111         0.11724
    107 ->114         0.11062
    107 ->115        -0.19762
    107 ->116         0.10048

Excited State  18:      Singlet-A      3.8473 eV  322.27 nm  f=0.0102  <S**2>=0.000
    100 ->108        -0.11388
    102 ->108        -0.10109
    103 ->109        -0.27319
    106 ->110        -0.11809
    106 ->112        -0.11822
    106 ->113         0.51769
    107 ->113         0.21612

Excited State  19:      Singlet-A      3.8549 eV  321.63 nm  f=0.0024  <S**2>=0.000
     99 ->108         0.30843
```

```
    100 ->108         0.10497
    102 ->108         0.46134
    106 ->110         0.24344
    106 ->111         0.15765
    106 ->113         0.16705
    106 ->114        -0.14835
    107 ->111         0.11453

Excited State  20:      Singlet-A      3.9769 eV  311.76 nm  f=0.0075  <S**2>=0.000
    100 ->108         0.40043
    101 ->108         0.38561
    102 ->108        -0.14062
    104 ->110         0.16704
    104 ->111        -0.20788
    104 ->114         0.23212

Excited State  21:      Singlet-A      4.0036 eV  309.68 nm  f=0.0012  <S**2>=0.000
     99 ->108         0.45223
    100 ->108         0.20952
    101 ->108        -0.17226
    102 ->108        -0.37208
    104 ->110        -0.10401
    104 ->111         0.12337
    104 ->114        -0.12207

Excited State  22:      Singlet-A      4.0236 eV  308.14 nm  f=0.0174  <S**2>=0.000
     99 ->108        -0.34703
    100 ->108         0.42728
    101 ->108        -0.18313
    104 ->110        -0.14813
    104 ->111         0.15251
    104 ->114        -0.18486
    107 ->108        -0.10367
    107 ->111         0.10629

Excited State  23:      Singlet-A      4.0352 eV  307.26 nm  f=0.0071  <S**2>=0.000
    101 ->108         0.51213
    104 ->110        -0.22645
    104 ->111         0.24842
    104 ->114        -0.27334

Excited State  24:      Singlet-A      4.0826 eV  303.69 nm  f=0.0437  <S**2>=0.000
    100 ->108         0.12461
```

```
    105 ->110         0.37487
    105 ->111        -0.30914
    105 ->114         0.28512
    106 ->112         0.11765
    107 ->111        -0.27445

Excited State  25:      Singlet-A      4.1260 eV  300.50 nm  f=0.0118  <S**2>=0.000
    105 ->110         0.19116
    105 ->111        -0.13731
    105 ->114         0.10749
    106 ->114         0.19980
    106 ->115        -0.18178
    107 ->111         0.45112
    107 ->114         0.26462
    107 ->115         0.11247

Excited State  26:      Singlet-A      4.1466 eV  299.00 nm  f=0.0189  <S**2>=0.000
    106 ->111         0.33461
    106 ->112         0.14320
    106 ->114         0.33701
    106 ->115        -0.28330
    106 ->116         0.13886
    107 ->111        -0.19825
    107 ->115        -0.20348

Excited State  27:      Singlet-A      4.2198 eV  293.81 nm  f=0.0035  <S**2>=0.000
     99 ->109         0.10364
    100 ->109        -0.28221
    101 ->109         0.32052
    104 ->112         0.16169
    104 ->113         0.21412
    105 ->112         0.32968
    105 ->113         0.20079
    106 ->111        -0.12458
    106 ->115        -0.10584

Excited State  28:      Singlet-A      4.2614 eV  290.94 nm  f=0.0004  <S**2>=0.000
     98 ->108         0.10179
    104 ->112         0.57938
    104 ->113         0.11625
    104 ->114        -0.13523
    105 ->112        -0.10597
    106 ->111         0.15049
```

```
    106 ->114         0.17086
    106 ->115         0.12787

Excited State  29:      Singlet-A      4.2663 eV  290.61 nm  f=0.0191  <S**2>=0.000
     98 ->108         0.47636
    101 ->109        -0.13001
    104 ->113        -0.10991
    106 ->111        -0.19640
    106 ->115        -0.24529
    106 ->116         0.14312
    107 ->114        -0.17997
    107 ->115        -0.11970

Excited State  30:      Singlet-A      4.2864 eV  289.25 nm  f=0.0008  <S**2>=0.000
     98 ->108         0.36645
    101 ->109         0.11653
    104 ->112        -0.28405
    104 ->113         0.38666
    106 ->111         0.12411
    106 ->114         0.13658
    106 ->115         0.17291

Excited State  31:      Singlet-A      4.2935 eV  288.78 nm  f=0.0095  <S**2>=0.000
     98 ->108         0.18765
    104 ->113        -0.28393
    105 ->112         0.43770
    106 ->111         0.15955
    106 ->114         0.11261
    106 ->115         0.25946
    106 ->116        -0.14065

Excited State  32:      Singlet-A      4.3233 eV  286.78 nm  f=0.0011  <S**2>=0.000
    100 ->109         0.19634
    101 ->109        -0.27310
    104 ->113         0.22673
    105 ->113         0.53854

Excited State  33:      Singlet-A      4.3313 eV  286.25 nm  f=0.0013  <S**2>=0.000
     98 ->108        -0.11524
    100 ->109         0.20505
    101 ->109        -0.22723
    104 ->113         0.28514
    105 ->112         0.36821
```

```
    105 ->113        -0.32257
    106 ->115        -0.11358

Excited State  34:      Singlet-A      4.3674 eV  283.88 nm  f=0.0966  <S**2>=0.000
     98 ->108        -0.20825
    102 ->109         0.39958
    103 ->112         0.10129
    105 ->114         0.15359
    106 ->112        -0.10810
    106 ->114         0.20000
    107 ->114        -0.31665

Excited State  35:      Singlet-A      4.4089 eV  281.21 nm  f=0.0170  <S**2>=0.000
    105 ->110         0.52122
    105 ->111         0.25786
    105 ->114        -0.29298
    107 ->114        -0.12569

Excited State  36:      Singlet-A      4.4366 eV  279.46 nm  f=0.0022  <S**2>=0.000
    103 ->110         0.44383
    103 ->111        -0.34763
    103 ->112         0.10101
    103 ->114         0.32213
    104 ->113         0.14596

Excited State  37:      Singlet-A      4.4688 eV  277.45 nm  f=0.0032  <S**2>=0.000
    102 ->109        -0.10476
    104 ->110         0.53189
    104 ->111         0.21161
    104 ->114        -0.23706
    104 ->115        -0.10223
    107 ->115        -0.13292
    107 ->116        -0.21676

Excited State  38:      Singlet-A      4.5070 eV  275.09 nm  f=0.0002  <S**2>=0.000
    104 ->110         0.21200
    107 ->115         0.29509
    107 ->116         0.57228

Excited State  39:      Singlet-A      4.5493 eV  272.53 nm  f=0.0660  <S**2>=0.000
    102 ->109        -0.30457
    103 ->112         0.55442
    103 ->114        -0.15246
```

```
Excited State  40:      Singlet-A      4.5739 eV  271.07 nm  f=0.0005  <S**2>=0.000
    106 ->115         0.32370
    106 ->116         0.60718

Excited State  41:      Singlet-A      4.6536 eV  266.42 nm  f=0.1929  <S**2>=0.000
    102 ->109         0.31599
    103 ->109        -0.13367
    103 ->112         0.17673
    103 ->113         0.36296
    105 ->111         0.20628
    105 ->115        -0.11318
    107 ->114         0.15720
    107 ->117         0.18613

Excited State  42:      Singlet-A      4.6673 eV  265.65 nm  f=0.0097  <S**2>=0.000
    105 ->111        -0.10411
    107 ->117         0.65570

Excited State  43:      Singlet-A      4.7003 eV  263.78 nm  f=0.0455  <S**2>=0.000
    102 ->109        -0.13365
    103 ->113        -0.22710
    105 ->111         0.31117
    105 ->114         0.36263
    105 ->115        -0.31665
    105 ->116         0.16755
    106 ->117        -0.15272

Excited State  44:      Singlet-A      4.7284 eV  262.21 nm  f=0.0131  <S**2>=0.000
    100 ->109         0.24487
    101 ->109         0.23260
    103 ->110         0.39429
    103 ->111         0.26068
    103 ->113        -0.15935
    103 ->114        -0.21070
    103 ->115        -0.12044
    104 ->115        -0.11808

Excited State  45:      Singlet-A      4.7317 eV  262.03 nm  f=0.0337  <S**2>=0.000
    100 ->109         0.14514
    101 ->109         0.15033
    102 ->109        -0.11790
    103 ->112        -0.13521
```

```
    103 ->113         0.22514
    104 ->111        -0.21960
    104 ->114        -0.21149
    104 ->115         0.29793
    104 ->116        -0.16144
    106 ->117         0.25672

Excited State  46:      Singlet-A      4.7668 eV  260.10 nm  f=0.0221  <S**2>=0.000
     99 ->109         0.12131
    100 ->109         0.32282
    101 ->109         0.21732
    103 ->110        -0.24941
    103 ->111        -0.15587
    103 ->112         0.10200
    103 ->113        -0.31929
    103 ->114         0.19455
    106 ->117         0.22624

Excited State  47:      Singlet-A      4.7784 eV  259.47 nm  f=0.0912  <S**2>=0.000
     99 ->109        -0.19318
    100 ->109         0.22187
    101 ->109         0.24755
    102 ->109        -0.12287
    103 ->110        -0.16081
    103 ->112        -0.16385
    103 ->113         0.25366
    103 ->114         0.10117
    104 ->111         0.11483
    104 ->114         0.16613
    104 ->115        -0.15838
    106 ->117        -0.20584
    107 ->114        -0.11010

Excited State  48:      Singlet-A      4.7804 eV  259.36 nm  f=0.0742  <S**2>=0.000
    100 ->109        -0.11254
    102 ->109        -0.10314
    104 ->111         0.18341
    104 ->114         0.20454
    104 ->115        -0.18543
    104 ->116         0.10397
    106 ->117         0.52767
    107 ->114        -0.10147
```

```
Excited State  49:      Singlet-A      4.8718 eV  254.49 nm  f=0.0075  <S**2>=0.000
     99 ->109         0.43233
    105 ->111        -0.23795
    105 ->114        -0.14505
    105 ->115        -0.35296
    105 ->116         0.19050

Excited State  50:      Singlet-A      4.9028 eV  252.88 nm  f=0.0112  <S**2>=0.000
     98 ->109         0.11993
     99 ->109         0.37548
    102 ->112         0.11299
    103 ->112        -0.12137
    105 ->111         0.22907
    105 ->114         0.19138
    105 ->115         0.31891
    105 ->116        -0.16944
    106 ->117        -0.10594
```

First 20 Excited States for 2-Zr as Predicted by TDDFT Using PW91PW91

```
Excited State   1:      Singlet-A      1.8029 eV  687.71 nm  f=0.0001  <S**2>=0.000
    107 ->108         0.70615

Excited State   2:      Singlet-A      1.9644 eV  631.16 nm  f=0.0001  <S**2>=0.000
    106 ->108         0.70256

Excited State   3:      Singlet-A      2.2538 eV  550.11 nm  f=0.0025  <S**2>=0.000
    104 ->108        -0.10781
    105 ->108         0.69737

Excited State   4:      Singlet-A      2.3286 eV  532.44 nm  f=0.0011  <S**2>=0.000
    107 ->109         0.69612

Excited State   5:      Singlet-A      2.5212 eV  491.76 nm  f=0.0054  <S**2>=0.000
    104 ->108        -0.11420
    106 ->109         0.68668

Excited State   6:      Singlet-A      2.6771 eV  463.13 nm  f=0.0089  <S**2>=0.000
    104 ->108         0.64380
    105 ->109         0.15389
    106 ->109         0.11820
    107 ->111         0.11493

Excited State   7:      Singlet-A      2.6964 eV  459.82 nm  f=0.0037  <S**2>=0.000
    103 ->108         0.13411
    104 ->108        -0.13650
    104 ->109        -0.13469
    105 ->109         0.65938

Excited State   8:      Singlet-A      2.7083 eV  457.80 nm  f=0.0000  <S**2>=0.000
    103 ->108         0.68943
    105 ->109        -0.12431

Excited State   9:      Singlet-A      2.9301 eV  423.14 nm  f=0.0003  <S**2>=0.000
    104 ->109         0.68648
    105 ->109         0.13589

Excited State  10:      Singlet-A      3.1867 eV  389.07 nm  f=0.0028  <S**2>=0.000
    107 ->110         0.68879
    107 ->111        -0.12987
```

```
Excited State  11:      Singlet-A      3.3291 eV  372.43 nm  f=0.0007  <S**2>=0.000
    106 ->110         0.70432

Excited State  12:      Singlet-A      3.3620 eV  368.78 nm  f=0.0220  <S**2>=0.000
    101 ->109         0.10838
    102 ->108        -0.41093
    103 ->109         0.48441
    107 ->111         0.26446

Excited State  13:      Singlet-A      3.3969 eV  364.99 nm  f=0.0007  <S**2>=0.000
    102 ->108         0.56555
    103 ->109         0.36973
    107 ->111         0.15243

Excited State  14:      Singlet-A      3.5553 eV  348.73 nm  f=0.0433  <S**2>=0.000
    103 ->109        -0.19545
    106 ->111         0.15004
    107 ->111         0.47040
    107 ->112        -0.37427
    107 ->113         0.17595

Excited State  15:      Singlet-A      3.5916 eV  345.20 nm  f=0.0015  <S**2>=0.000
    101 ->108        -0.12859
    106 ->111         0.66250

Excited State  16:      Singlet-A      3.6093 eV  343.51 nm  f=0.0014  <S**2>=0.000
    105 ->110         0.69785

Excited State  17:      Singlet-A      3.6430 eV  340.34 nm  f=0.0017  <S**2>=0.000
    101 ->108         0.68033
    106 ->111         0.11103

Excited State  18:      Singlet-A      3.6969 eV  335.38 nm  f=0.0054  <S**2>=0.000
    107 ->111         0.12852
    107 ->112         0.46579
    107 ->113         0.49221

Excited State  19:      Singlet-A      3.7578 eV  329.94 nm  f=0.0045  <S**2>=0.000
    102 ->109         0.65793
    107 ->113         0.11774
    107 ->114        -0.14731

Excited State  20:      Singlet-A      3.7850 eV  327.57 nm  f=0.0102  <S**2>=0.000
```

100 ->108	0.57681
102 ->109	-0.14242
107 ->112	-0.13222
107 ->113	0.26386

First 20 Excited States for 2-Zr as Predicted by TDDFT Using B3LYP

```
 Excited State   1:      Singlet-A      2.0331 eV  609.83 nm  f=0.0012  <S**2>=0.000
     107 ->108         0.69299

 Excited State   2:      Singlet-A      2.3438 eV  528.98 nm  f=0.0002  <S**2>=0.000
     106 ->108         0.64818
     107 ->109        -0.24432

 Excited State   3:      Singlet-A      2.4725 eV  501.46 nm  f=0.0009  <S**2>=0.000
     106 ->108         0.21829
     106 ->109        -0.18077
     107 ->109         0.63592

 Excited State   4:      Singlet-A      2.5332 eV  489.43 nm  f=0.0028  <S**2>=0.000
     103 ->109         0.26388
     106 ->108         0.15867
     106 ->109         0.60053
     107 ->109         0.15641

 Excited State   5:      Singlet-A      2.5997 eV  476.92 nm  f=0.0031  <S**2>=0.000
     104 ->109        -0.26762
     105 ->108        -0.22573
     105 ->109         0.58638

 Excited State   6:      Singlet-A      2.7907 eV  444.28 nm  f=0.0028  <S**2>=0.000
     104 ->108        -0.13392
     104 ->109         0.53707
     105 ->108        -0.40466
     105 ->109         0.10485

 Excited State   7:      Singlet-A      2.8073 eV  441.65 nm  f=0.0011  <S**2>=0.000
     104 ->108        -0.25474
     104 ->109         0.24269
     105 ->108         0.49991
     105 ->109         0.33618

 Excited State   8:      Singlet-A      2.9927 eV  414.29 nm  f=0.0058  <S**2>=0.000
     104 ->108         0.61311
     104 ->109         0.25202
     105 ->108         0.13258
     107 ->112         0.10580
```

```
Excited State   9:      Singlet-A      3.1539 eV  393.12 nm  f=0.0007  <S**2>=0.000
    103 ->108         0.69798

Excited State  10:      Singlet-A      3.6362 eV  340.97 nm  f=0.0307  <S**2>=0.000
    103 ->109         0.58154
    106 ->109        -0.26920
    107 ->110         0.13754
    107 ->111        -0.15150
    107 ->112         0.11368

Excited State  11:      Singlet-A      3.7702 eV  328.86 nm  f=0.0111  <S**2>=0.000
    103 ->109        -0.12042
    107 ->110         0.66918
    107 ->111        -0.10610

Excited State  12:      Singlet-A      3.8989 eV  318.00 nm  f=0.0108  <S**2>=0.000
    102 ->108         0.60067
    102 ->109        -0.11388
    106 ->110         0.23147
    106 ->111        -0.16017
    106 ->112         0.11319

Excited State  13:      Singlet-A      3.9162 eV  316.59 nm  f=0.0036  <S**2>=0.000
    102 ->108        -0.31993
    106 ->110         0.49452
    106 ->111        -0.28697
    106 ->112         0.19151
    106 ->113        -0.10654

Excited State  14:      Singlet-A      3.9898 eV  310.75 nm  f=0.0008  <S**2>=0.000
    101 ->108         0.63700
    102 ->109         0.13276
    106 ->110         0.10991
    107 ->115         0.19599

Excited State  15:      Singlet-A      4.0385 eV  307.00 nm  f=0.0016  <S**2>=0.000
    100 ->109        -0.10087
    101 ->108        -0.16335
    102 ->109         0.24665
    106 ->110         0.39458
    106 ->111         0.30783
    106 ->112        -0.26195
    106 ->113         0.14635
```

```
    107 ->115         0.12658

Excited State  16:      Singlet-A      4.0546 eV  305.78 nm  f=0.0498  <S**2>=0.000
    106 ->115         0.14837
    107 ->110         0.13883
    107 ->111         0.62989

Excited State  17:      Singlet-A      4.0828 eV  303.68 nm  f=0.0030  <S**2>=0.000
    100 ->108         0.17895
    100 ->109        -0.21038
    101 ->108        -0.12682
    102 ->109         0.51769
    106 ->110        -0.13938
    106 ->111        -0.23096
    106 ->112         0.16976

Excited State  18:      Singlet-A      4.1090 eV  301.74 nm  f=0.0001  <S**2>=0.000
     99 ->108        -0.16710
    101 ->108        -0.11845
    102 ->109        -0.13173
    106 ->111        -0.12455
    107 ->112         0.12756
    107 ->114         0.29516
    107 ->115         0.50562

Excited State  19:      Singlet-A      4.1720 eV  297.18 nm  f=0.0044  <S**2>=0.000
    100 ->108         0.64752
    100 ->109         0.10336
    102 ->109        -0.13426

Excited State  20:      Singlet-A      4.2329 eV  292.90 nm  f=0.0168  <S**2>=0.000
    105 ->110         0.35518
    105 ->111        -0.25016
    105 ->112         0.14153
    106 ->114        -0.10387
    106 ->115        -0.13552
    107 ->111         0.10370
    107 ->112         0.36268
    107 ->113        -0.13230
    107 ->115        -0.19735
```

First 20 Excited States for 2-Hf as Predicted by TDDFT Using PW91PW91

```
Excited State   1:      Singlet-A      2.0081 eV  617.43 nm  f=0.0005  <S**2>=0.000
    107 ->108         0.70256

Excited State   2:      Singlet-A      2.1266 eV  583.02 nm  f=0.0001  <S**2>=0.000
    106 ->108         0.68780
    107 ->109        -0.12422

Excited State   3:      Singlet-A      2.3531 eV  526.91 nm  f=0.0009  <S**2>=0.000
    106 ->108         0.13352
    107 ->109         0.68150

Excited State   4:      Singlet-A      2.4323 eV  509.75 nm  f=0.0027  <S**2>=0.000
    104 ->108        -0.10122
    105 ->108         0.69466

Excited State   5:      Singlet-A      2.4863 eV  498.67 nm  f=0.0051  <S**2>=0.000
    106 ->109         0.69039

Excited State   6:      Singlet-A      2.6729 eV  463.86 nm  f=0.0028  <S**2>=0.000
    104 ->109        -0.13966
    105 ->109         0.68577

Excited State   7:      Singlet-A      2.8636 eV  432.97 nm  f=0.0087  <S**2>=0.000
    104 ->108         0.63846
    104 ->109        -0.19259
    107 ->111        -0.12640

Excited State   8:      Singlet-A      2.8835 eV  429.98 nm  f=0.0009  <S**2>=0.000
    103 ->108         0.68417
    104 ->109        -0.11810

Excited State   9:      Singlet-A      2.9370 eV  422.14 nm  f=0.0013  <S**2>=0.000
    103 ->108         0.13524
    104 ->108         0.17186
    104 ->109         0.64890
    105 ->109         0.11999

Excited State  10:      Singlet-A      3.2032 eV  387.06 nm  f=0.0019  <S**2>=0.000
    107 ->110         0.69553

Excited State  11:      Singlet-A      3.2989 eV  375.84 nm  f=0.0004  <S**2>=0.000
```

```
    106 ->110         0.70582

Excited State  12:      Singlet-A      3.3605 eV  368.94 nm  f=0.0251  <S**2>=0.000
    101 ->109         0.15150
    103 ->109         0.61957
    107 ->111        -0.25212

Excited State  13:      Singlet-A      3.5712 eV  347.18 nm  f=0.0044  <S**2>=0.000
    102 ->108         0.62944
    105 ->110        -0.12836
    107 ->111         0.20701
    107 ->112         0.12846

Excited State  14:      Singlet-A      3.5859 eV  345.76 nm  f=0.0217  <S**2>=0.000
    102 ->108        -0.19154
    105 ->110        -0.22307
    106 ->111         0.46149
    107 ->111         0.33666
    107 ->112         0.24345

Excited State  15:      Singlet-A      3.6002 eV  344.38 nm  f=0.0014  <S**2>=0.000
    102 ->108         0.11179
    105 ->110         0.63246
    106 ->111         0.26930

Excited State  16:      Singlet-A      3.6160 eV  342.88 nm  f=0.0191  <S**2>=0.000
    102 ->108         0.19535
    105 ->110        -0.16945
    106 ->111         0.42713
    107 ->111        -0.31051
    107 ->112        -0.34527

Excited State  17:      Singlet-A      3.7536 eV  330.31 nm  f=0.0044  <S**2>=0.000
    102 ->109         0.67665
    107 ->112        -0.11488

Excited State  18:      Singlet-A      3.8064 eV  325.73 nm  f=0.0108  <S**2>=0.000
    101 ->108         0.55000
    107 ->111        -0.17445
    107 ->112         0.31802
    107 ->113         0.16235

Excited State  19:      Singlet-A      3.8231 eV  324.30 nm  f=0.0134  <S**2>=0.000
```

```
     101 ->108        -0.24266
     101 ->109        -0.13761
     102 ->109         0.14400
     106 ->112         0.47988
     107 ->111        -0.17059
     107 ->112         0.28753
     107 ->113         0.16209

Excited State  20:      Singlet-A      3.8371 eV  323.12 nm  f=0.0092  <S**2>=0.000
     101 ->108         0.33472
     101 ->109         0.12707
     105 ->111        -0.11813
     106 ->111        -0.10895
     106 ->112         0.48011
     107 ->111         0.13416
     107 ->112        -0.20298
     107 ->113        -0.17970
```

First 20 Excited States for 2-Hf as Predicted by TDDFT Using B3LYP

```
Excited State   1:      Singlet-A      2.3167 eV  535.18 nm  f=0.0030  <S**2>=0.000
    107 ->108         0.69177

Excited State   2:      Singlet-A      2.4497 eV  506.12 nm  f=0.0005  <S**2>=0.000
    103 ->109         0.10480
    106 ->108        -0.33998
    106 ->109         0.14689
    107 ->109         0.57584

Excited State   3:      Singlet-A      2.4894 eV  498.05 nm  f=0.0025  <S**2>=0.000
    103 ->109         0.26086
    106 ->109         0.60195
    107 ->109        -0.22745

Excited State   4:      Singlet-A      2.5740 eV  481.68 nm  f=0.0011  <S**2>=0.000
    104 ->109        -0.21416
    105 ->109         0.51781
    106 ->108         0.31918
    106 ->109         0.10704
    107 ->109         0.21680

Excited State   5:      Singlet-A      2.5994 eV  476.97 nm  f=0.0025  <S**2>=0.000
    105 ->109        -0.38333
    106 ->108         0.51637
    107 ->109         0.24227

Excited State   6:      Singlet-A      2.8220 eV  439.34 nm  f=0.0001  <S**2>=0.000
    104 ->108        -0.12250
    104 ->109         0.64292
    105 ->109         0.21798

Excited State   7:      Singlet-A      2.9693 eV  417.55 nm  f=0.0032  <S**2>=0.000
    104 ->108        -0.14536
    105 ->108         0.66998
    105 ->109         0.12301

Excited State   8:      Singlet-A      3.2085 eV  386.42 nm  f=0.0085  <S**2>=0.000
    104 ->108         0.64916
    104 ->109         0.12499
    105 ->108         0.13260
    107 ->112         0.12889
```

```
Excited State   9:      Singlet-A      3.3210 eV  373.34 nm  f=0.0004  <S**2>=0.000
    103 ->108         0.69828

Excited State  10:      Singlet-A      3.6559 eV  339.13 nm  f=0.0458  <S**2>=0.000
    103 ->109         0.59616
    106 ->109        -0.27563
    107 ->111        -0.13409
    107 ->112         0.12655

Excited State  11:      Singlet-A      3.8097 eV  325.44 nm  f=0.0072  <S**2>=0.000
    107 ->110         0.67847
    107 ->111         0.13836

Excited State  12:      Singlet-A      3.9540 eV  313.56 nm  f=0.0007  <S**2>=0.000
    102 ->109         0.11172
    106 ->110         0.65188
    106 ->111         0.21113

Excited State  13:      Singlet-A      4.0254 eV  308.01 nm  f=0.0017  <S**2>=0.000
    100 ->109        -0.19499
    102 ->108        -0.20443
    102 ->109         0.59630
    106 ->110        -0.16566

Excited State  14:      Singlet-A      4.1251 eV  300.56 nm  f=0.0072  <S**2>=0.000
    102 ->108         0.38419
    106 ->110        -0.13497
    106 ->111         0.34572
    106 ->112        -0.26456
    107 ->111         0.31638

Excited State  15:      Singlet-A      4.1347 eV  299.86 nm  f=0.0046  <S**2>=0.000
    102 ->108         0.46001
    102 ->109         0.23936
    106 ->110         0.13185
    106 ->111        -0.32955
    106 ->112         0.25488

Excited State  16:      Singlet-A      4.1562 eV  298.31 nm  f=0.0474  <S**2>=0.000
    101 ->108        -0.11305
    102 ->108        -0.24976
    106 ->111        -0.16524
```

```
    106 ->112         0.11842
    107 ->110        -0.12442
    107 ->111         0.56365

Excited State  17:      Singlet-A      4.1933 eV  295.67 nm  f=0.0019  <S**2>=0.000
    101 ->108         0.67730

Excited State  18:      Singlet-A      4.2971 eV  288.53 nm  f=0.0063  <S**2>=0.000
    101 ->109         0.10301
    105 ->110         0.61149
    105 ->111         0.28187
    107 ->112        -0.13130

Excited State  19:      Singlet-A      4.3955 eV  282.07 nm  f=0.0126  <S**2>=0.000
    100 ->108         0.26634
    101 ->109        -0.25536
    105 ->110         0.13995
    106 ->115        -0.23070
    107 ->112         0.48813

Excited State  20:      Singlet-A      4.4277 eV  280.02 nm  f=0.0065  <S**2>=0.000
     99 ->108         0.21746
    100 ->108         0.45435
    104 ->110        -0.13203
    106 ->111         0.23066
    106 ->112         0.25075
    107 ->112        -0.11107
    107 ->115        -0.21860
```

References:

1. D. F. Shriver and M. A. Drezdon, John Wiley & Sons, New York, 2nd edn., 1986, p. 326.

2. B. J. Burger and J. E. Bercaw, in *Experimental Organometallic Chemistry*, eds. A. L. Wayda and M. Y. Darensbourg, American Chemical Society, Washington, DC, 1987, p. 79-98.

3. A. B. Pangborn, M. A. Giardello, R. H. Grubbs, R. K. Rosen and F. J. Timmers, *Organometallics*, 1996, **15**, 1518-1520.

4. D. S. Glueck, J. Wu, F. J. Hollander and R. G. Bergman, *J. Am. Chem. Soc.*, 1991, **113**, 2041-2054.

5. D. S. Glueck, F. J. Hollander and R. G. Bergman, *J. Am. Chem. Soc.*, 1989, **111**, 2719-2721.

6. A. M. Baranger and R. G. Bergman, *J. Am. Chem. Soc.*, 1994, **116**, 3822-3835.

7. A. M. Baranger, F. J. Hollander and R. G. Bergman, *J. Am. Chem. Soc.*, 1993, **115**, 7890-7891.

8. V. V. Burlakov, T. Beweries, V. S. Bogdanov, P. Arndt, W. Baumann, P. V. Petrovskii, A. Spannenberg, K. A. Lyssenko, V. B. Shur and U. Rosenthal, *Organometallics*, 2009, **28**, 2864-2870.

9. P. Binger, P. Müller, F. Langhauser, F. Sandmeyer, P. Philipps, B. Gabor and R. Mynott, *Chem. Ber.*, 1993, **126**, 1541-1550.

10. P. A. S. Smith and J. H. Boyer, *Organic Syntheses*, **31**, 14-17.

11. G. Sheldrick, *Acta Crystallographica Section A*, 2008, **A64**, 112-122.

12. R. R. Schrock, L. G. Sturgeoff and P. R. Sharp, *Inorg. Chem.*, 1983, **22**, 2801-2806.

13. Z.-W. Li, A. Yeh and H. Taube, *Inorg. Chem.*, 1994, **33**, 2874-2881.

14. J. C. Peters, J.-P. F. Cherry, J. C. Thomas, L. Baraldo, D. J. Mindiola, W. M. Davis and C. C. Cummins, *J. Am. Chem. Soc.*, 1999, **121**, 10053-10067.

15. R. R. Schrock, R. M. Kolodziej, A. H. Liu, W. M. Davis and M. G. Vale, *J. Am. Chem. Soc.*, 1990, **112**, 4338-4345.

16. R. Cordone, W. D. Harman and H. Taube, *J. Am. Chem. Soc.*, 1989, **111**, 2896-2900.

17. M. J. Frisch, G. W. Trucks and H. B. Schlegel, et al., Gaussian, Inc., Wallingford, CT, 2009.

18. T. H. Dunning Jr. and P. J. Hay, in *Modern Theoretical Chemistry*, ed. H. F. S. III, Plenum, New York, 1976, vol. 3, p. 1-28

19. D. Andrae, U. Haeussermann, M. Dolg, H. Stoll and H. Preuss, *Theor. Chem. Acc.*, 1990, **77**, 123-141.

20. U. Wedig, M. Dolg, H. Stoll and H. Preuss, in *Quantum Chemistry: The Challenge of Transition Metals and Coordination Chemistry*, ed. A. Veillard, Springer, 1986, p. 79-90.

21. G. A. Petersson, A. Bennett, T. G. Tensfeldt, M. A. Al-Laham, W. A. Shirley and J. Mantzaris, *J. Chem. Phys.*, 1988, **89**, 2193-2218.

22. G. A. Petersson and M. A. Al-Laham, *J. Chem. Phys.*, 1991, **94**, 6081-6090.

23. A. D. Becke, *J. Chem. Phys.*, 1993, **98**, 5648-5652.

24. A. D. Becke, *Phys. Rev. A: At. Mol. Opt. Phys.*, 1988, **38**, 3098-3100.

25. C. Lee, W. Yang and R. G. Parr, *Phys. Rev. B: Condens. Matter*, 1988, **37**, 785-789.

26. B. Miehlich, A. Savin, H. Stoll and H. Preuss, *Chem. Phys. Lett.*, 1989, **157**, 200-206.

27. J. P. Perdew, eds. P. Ziesche and H. Eschrig, Akademie Verlag, Berlin, 1991, p. 11.

28. J. P. Perdew, J. A. Chevary, S. H. Vosko, K. A. Jackson, M. R. Pederson, D. J. Singh and C. Fiolhais, *Phys. Rev. B: Condens. Matter*, 1992, **46** 6671-6687.

29. J. P. Perdew, J. A. Chevary, S. H. Vosko, K. A. Jackson, M. R. Pederson, D. J. Singh and C. Fiolhais, *Phys. Rev. B: Condens. Matter*, 1993, **48**, 4978.

30. J. P. Perdew, K. Burke and Y. Wang, *Phys. Rev. B: Condens. Matter*, 1996, 16533-16539.

31. K. Burke, J. P. Perdew and Y. Wang, in *Electronic Density Functional Theory: Recent Progress and New Directions*, eds. J. F. Dobson, G. Vignale and M. P. Das, Plenum, New York, 1998.

32. R. Bauernschmitt and R. Ahlrichs, *Chem. Phys. Lett.*, 1996, **256**, 454-464.

33. C. V. Caillie and R. D. Amos, *Chem. Phys. Lett.*, 2000, **317**, 159-164.

34. M. E. Casida, C. Jamorski, K. C. Casida and D. R. Salahub, *J. Chem. Phys.*, 1998, **108**, 4439-4449.

35. F. Furche and R. Ahlrichs, *J. Chem. Phys.*, 2002, **117**, 7433-7447.

36. H. B. Schlegel, S. S. Iyengar, J. M. M. X. Li, G. A. Voth, G. E. Scuseria and M. J. Frisch, *J. Chem. Phys.*, 2002, **117**, 8694-8704.

37. G. W. T. J. R. Cheeseman, T. A. Keith, and M. J. Frisch, *J. Chem. Phys.*, 1996, **104**, 5497-5509.

38. F. London, *J. Phys. Radium*, 1937, **8**, 397-409.

39. R. McWeeny, *Phys. Rev.*, 1962, **126** 1028.

40. R. Ditchfield, *Mol. Phys.*, 1974, **27**, 789-807.

41. K. Wolinski, J. F. Hilton and P. Pulay, *J. Am. Chem. Soc.*, 1990, **112**, 8251-8260.

42. J. Gauss, *Chem. Phys. Lett.*, 1992, **191**, 614-620.

43. J. Gauss, *J. Chem. Phys.*, 1993, **99**, 3629-3643.

44. J. Gauss, *PCCP*, 1995, **99**, 1001-1008.